Politecnico di Torino

Master's Degree in Electrical Engineering

A.Y. 2024/2025

Techno-Economic Optimization and Design of a Large-Scale Photovoltaic System

MASTER THESIS

Politecnico di Torino

Supervisor: Filippo Spertino

Author: Samuele Sabatini

Co-Supervisor:
Francisco Diaz-Gonzalez

March 12, 2025

"An engineer measures with a micrometer,
marks with chalk, and cuts with an axe."

Contents

List of Figures

List of Tables

Introduction

This project of thesis focuses on the design and techno-economic optimisation of a large scale[1], grid-connected photovoltaic plant in response to the increasing demand for sustainable energy that derives from climate objective agreements. While maintaining adherence to technical, the project seeks to optimize energy output and cost-effectiveness that are key parameters in order to attract potential private or public investments.

The structure of the thesis is the following:

- Chapter 1: Fundamentals of Photovoltaic Technology and System Topologies – Examines the properties of solar radiation, the fundamentals of photovoltaic energy conversion, and the several types of photovoltaic modules. Additionally, it covers site selection, and gives a summary of the system design and the choice of essential parts.
- Chapter 2: System Sizing and Plant Productivity Estimate - After going over elements, such as the nominal power ratio, inverter DC input power, and AC active power calculation; focuses on the engineering aspects of system sizing, including : module voltage range, module current, and string design. It ends with a calculation of the annual energy production backed by simulation methods.
- Chapter 3: Design and Optimization of Grid-Connected Power Plants - Examines land usage, cable and protection sizing, and the design of electrical protection systems in order to safely connect the plant to the grid.
- Chapter 4: Economic and Environmental Evaluation - Covers Levelized Cost of Energy, economical sustainability of the plant considering Italian electricity market and an environmental impact assessment

Basic components of a photovoltaic system include a generator (photovoltaic modules), a support structure for ground, building, or other construction installation of the modules, a power control and conditioning system, a potential energy storage unit, electrical modules with switching and protection devices, and the cables that connect them.

The photovoltaic plant converts solar radiation instantly and directly into electrical energy without burning any fossil fuel.

The photovoltaic technology exploits the photovoltaic effect that consists in the fact that if a doped semiconductor is exposed to sunlight it produces electricity.

The main advantages of this technology are[12]:

- Distributed generation (in opposition to concentrated generation of traditional thermal plant);

[1] Often called utility-scale.

- Absence of CO_2 emissions and other pollutants;
- Reliability of the system (since there are no rotating parts);
- Operative life that goes from 20 to 30 years;
- Low maintenance costs;
- Null marginal cost of the primary energy source (sun/ sunlight);
- Modular design: scaling up plant power by adding modules to meet user needs.

Overview of Italian Energy and Climate Policy

The following information about the Italian energy policy are taken from the International Energy Agency(IEA)[13] report about Italy and from the lessons of:"E-transition Sustainability and Economics"[9].

Energy sector management in Italy

In Italy, legislative authority over energy production, transport, and distribution is shared between the central government and the regions, with regional powers constrained by national laws. Coordination between national and regional energy policies is facilitated through the State-Region Conference.

In 2021, the energy-related responsibilities previously managed by the Ministry of Economic Development were transferred to the newly established Ministry of Ecological Transition (MiTE). In order to encourage the shift to a net-zero carbon economy, this ministry was established to coordinate energy and climate policies. MiTE changed its name in 2022, becoming the Ministry of the environment and energy security.

Italy's energy strategy, try to follow European Union directives, focuses on decarbonization by increasing renewable energy capacity installed, promoting electrification, and improving energy efficiency. During the early 2010s, all Italian regions and autonomous provinces formulated regional energy-environmental plans to define energy policy goals and reduce greenhouse gas emissions. However, by June 2022, only two regions(Piedmont and Sicily) had revised their plans following the adoption of the National Energy and Climate Plan (NECP). Three other regions (Apulia, Campania, and Sardinia) had initiated the update process. The slow progress in updating regional plans has created a misalignment with national and EU energy and climate objectives, impeding effective policy implementation.

The Ministry of Ecological Transition (MiTE) oversees the coordination of several organisations that make up the Italian energy information system, including ARERA, GSE, RSE, ENEA, and Terna. Because data must be shared and approved across multiple entities, this fragmented structure adds to the administrative complexity. There is a pressing need for clearer delineation of roles

and formal agreements to improve coordination. Additionally, MiTE faces operational challenges due to limited human and financial resources, which hinder its ability to effectively oversee the energy information system.

Policies and Targets for 2030

Italy's strategy for reaching its 2030 goals for greenhouse gas emissions, the use of renewable energy, and energy efficiency is outlined in the National Energy and Climate Plan (NECP).

The NECP in 2023 was improved to be compliant with the project: "Fit for 55", which aim to cut net GHG emissions by 55% by 2030.

To reach this objectives the Ecological Transition Plan (ETP) has been developed, one of its ambitious targets is to generate 72% of electricity from renewable sources as part of Italy's strategy to meet its climate commitments.

The NECP identifies 101 specific policies and measures, to respect them is estimated that a huge investment of about 183 billion € will be needed by 2030 to realize this plans, to put things in perspective it is more than 1 percent of GDP per year.

Key areas of focus include increasing renewable energy capacity installed, particularly wind and solar power (that are the most available), electricity storage technologies (e.g. batteries) to compensate the intermittence of renewable generation, increasing energy efficiency in buildings and enhancing public transportation.

The plan also explores the potential of hydrogen as a clean energy source, though its use is expected to be limited to hard to abate sectors (e.g. steel production, concrete production, chemical plants, air transport etc.)

One of Italy's major goals is to phase out coal by 2025. This goal has been put in the background for uncertainty due to energy security concerns following Russia's decision to cut gas supplies in June 2022.

In response, Italy temporarily reopened some coal-based power generation plants increasing its reliance on coal power, which led to a short-term rise in GHGs emissions, marking a setback in its decarbonization efforts.

The NECP relies on well-established policy tools, such as tax incentives for energy-efficient building renovations and zero-emission vehicles, subsidies for renewable energy projects, and biofuel quotas.

However, it focus less emphasis on promoting behavioral changes to lower energy consumption, a tactic that the International IEA and the EU's REPowerEU plan both strongly support.

This gap highlights an area where Italy could further strengthen its approach to achieving its climate and energy goals.

In Tab.1 are presented the goals in terms of GHGs reduction, energy consumption reduction and electricity generation share from renewable energy sources (RES).

Category	Subcategory	2020 Status	2030 (NECP)	2030 (Fit for 55)
GHG Emissions	Net GHG emissions vs. 1990 (incl. removals)	-32%		-55%
	$CO_{2,eq}$ vs. 2005 (Effort Sharing Regulation)	-25%	-33%	-43.7%
Energy Efficiency	Primary energy consumption	6084 PJ	5238 PJ	4681 PJ
	Final energy consumption	4742 PJ	4346 PJ	3936 PJ
Renewable Energy Share	Overall target	19%	30%	36.7%
	Electricity	36%	55.4%	62-65%
	Heating and cooling	19.7%	33.9%	40%
	Transport	10%	21.6%	38%
Renewable Electricity (ETP Target)				72%
Cross-border Electricity Interconnection		8%	10%	
Energy Dependence		77.7%	75.4%	

Table 1: Italy's 2030 energy and climate targets.

At the current pace, the objectives for 2030 should be reached, but the fit for 55 objective will be very challenging to achieve. In fact, the primary energy consumption will decrease because low efficiency energy vector will be replaced with electricity, that is the most efficient way of transporting and utilizing energy.

Long-term Strategies for 2050

The long term strategy (LTS) shows different pathways to reach carbon neutrality by 2050 and could be further modified if new technologies are developed in the next year.

In order to achieve this, the LTS predicts that more than twice as much electricity will need to be produced by 2050, with 95 percent coming from renewable sources. Additionally, there will need to be a massive electrification, with electricity covering more than half of energy demand, and even more in the buildings and transportation sectors; new forms of flexibility, such as Power-to-X; a gradual replacement of natural gas with hydrogen and other synthetic fuels; and a shift in transportation habits.

All the objectives will be very challenging, but, among all, the most difficult to achieve will be the very high share of electricity generation from renewable sources, as right now there is no country in the world, with energy consumption comparable to that of Italy, capable of doing so in an economically sustainable manner, this is mainly due to the fact that the electricity storage on large scale has still huge costs and technical limitation.

1 Fundamentals of Photovoltaic Technology and System Topology Selection

1.1 Principles of Photovoltaic Energy Conversion

The conversion of solar radiation into electrical energy in photovoltaic (PV) solar modules occurs when the solar radiation composed by photons hits the semiconductor material (silicon), this phenomenon is known as "photovoltaic effect". the photovoltaic effect does not happen when the silicon is pure, but when it is doped, that is when artificially placed in one of the two following particular conditions:

- The semiconductor material (silicon) incorporates a P-type atom (e.g. boron);
- The semiconductor material (silicon) incorporates an N-type atom (e.g. phosphorus).

A semiconductor's doping operation consists in adding atoms other than silicon.

To gain a deeper comprehension of how they operate, it is useful to analyze the atomic structure of silicon atoms in a solar cell. Each silicon atom is surrounded by other silicon atoms, sharing one of its four valence electrons in the outermost orbitals with each of them.

Introducing into the crystalline lattice an atom with 3 electrons in the outer orbitals (for instance, a boron atom) creates an empty space in the lattice due to the lack of one electron compared to the surrounding silicon atoms (which have 4 electrons). This empty space is called a hole in the valence band: the atom is called acceptor and the semiconductor is P-type.

Similarly, introducing into the lattice an atom with 5 electrons in the outer orbitals (e.g. a phosphorus) results in an excess electron. In this case the atom is called donor and the semiconductor is N-type.

In Fig.1 there is a schematic to visualize this molecular configuration.

Putting two crystals of P-type and N-type silicon into contact, they form a P-N junction, as shown in Fig.2. The holes (empty spaces in the orbitals) in the P-type crystal tend to move into the N-type crystal; similarly, the excess electrons in the N-type crystal tend to move towards the P-type crystal creating a so called "depletion zone".

This phenomenon continues until the electric potential generated by the movement of charges balances the diffusion motion.

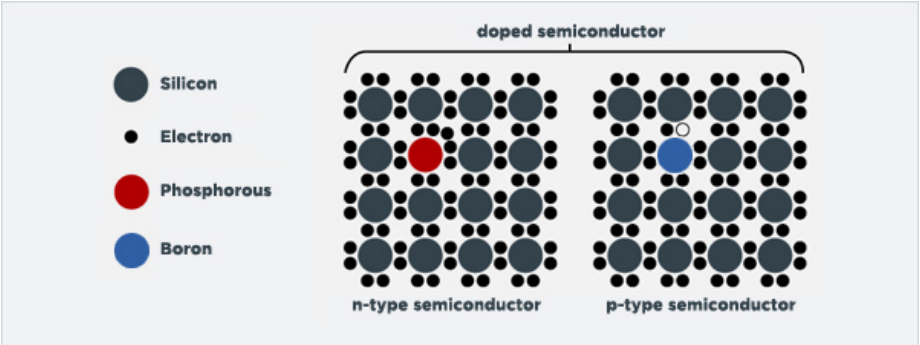

Figure 1: Doped silicon P-type and N-type junction[1].

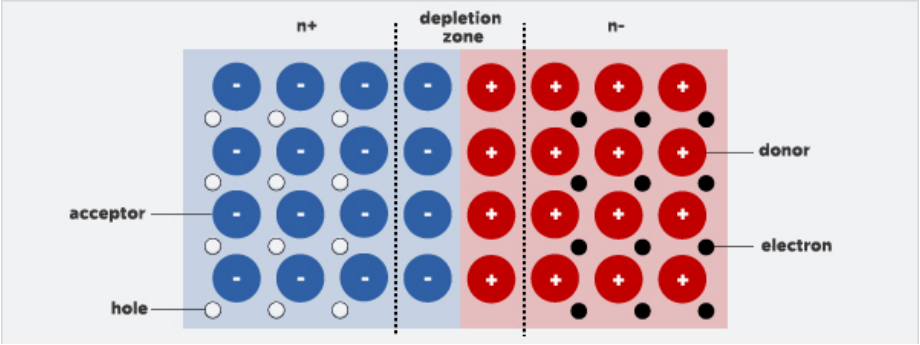

Figure 2: PN-junction[2]

In conclusion, when a photon with sufficient energy (higher than the bangap) hits the silicon in the depletion zone the excited electron go towards the P-type side of the PN junction, while the holes go toward the N-type side.

Connecting an external circuit between the two side previously mentioned a direct current is created.

Photovoltaic Modules: Technologies and Materials

The base unit of a PV module is the solar cell, obtained starting from silicon using thermal power, doping the silicon and finally using some mechanical processing.

For clarity of exposition and to avoid misunderstandings, the components of a photovoltaic plant are presented from the smallest to the biggest, the definition adopted in this section will be extensively used in the following chapters.

1. Photovoltaic cell: it is the fundamental component of the module, made of semiconductor material (typically silicon). This is where the photovoltaic effect occurs;

2. Photovoltaic module: it is a productive unit composed of several photovoltaic cells connected in series and/or parallel, enclosed in a protective frame and covered with glass. The modules are the primary components that convert solar energy into electrical power;

3. Photovoltaic String: it is a series connection of photovoltaic modules. The series connection increases the output voltage of the group, making it compatible with the inverter input voltage;

4. Photovoltaic array: (photovoltaic set): it is a portion of the plant composed of a set of strings or module sets, arranged to maximize solar exposure and optimize energy output of modules. It can be subdivided into smaller units to facilitate management and maintenance;

5. Photovoltaic plant: it is the complete system that includes all the subsystems necessary for producing and integrating solar energy into the electrical grid. It comprises arrays, inverters, power transformer (when is present), support structures, monitoring systems, and electrical connections.

The production of the module is very energy intensive, as between 200-300 kWh[2] are needed to obtain 1 kg of solar grade silicon; but with 1 kg of solar grade silicon an energy production of about 250 kWh per year can be expected, thus energy costs are paid for in just over a year.

There are different photovoltaic technologies, with some originating during the early days of space missions and others being more recently developed. These different types of modules posses distinct properties, costs, and characteristics.

The description of the different technology was taken combining information from a brief report produced by Pennsylvania State University [14] and from the notes taken during the course :"Renwable Energy Systems", by Professor Filippo Spertino, Politecnico di Torino A.Y. 2023 [3].

Monocrystalline Silicon Modules

Monocrystalline silicon solar cells are the oldest type of solar cells.

The monocrystalline silicon solar cells were first developed in 1954 by researchers Daryl Chapin, Calvin Fuller, and Gerald Pearson at Bell Laboratories in the United States.

This first photovoltaic cell had an efficiency of about 6% and represented a major breakthrough compared to previous cells based on materials like selenium, which had much lower efficiencies.

The idea of photovoltaics had already been known since the 19th century, thanks to the discovery of the photovoltaic effect by Alexandre Edmond Becquerel in 1839, but it was only with the development of silicon semiconductor technology (used in transistors) that truly functional solar cells became possible.

[2]With the "block casting" technique used for poly-crystalline silicon the energy needed can be reduced to 60 to 65 kWh/kg

The first applications of monocrystalline silicon cells were in space satellites, particularly with the Vanguard I satellite (1958), which used solar panels to power its communication systems. Since then, the technology has evolved, reaching modern cells with efficiencies exceeding 24%.

The production of high-purity silicon for solar cells is a multi-stage process that begins with the extraction of metallurgical-grade silicon (MG-Si) and culminates in the fabrication of monocrystalline silicon wafers. This process is energy-intensive but essential for the photovoltaic and electronics industries.

Stage 1: Production of Metallurgical-Grade Silicon (MG-Si)

The first stage involves the reduction of quartz (SiO_2) in a graphite arc furnace at high temperatures (1800–2000°C). The chemical reaction is as follows:

$$SiO_2 + 2C \rightarrow Si + 2CO.$$

This process yields silicon with a purity of 98–99%, known as metallurgical-grade silicon (MG-Si). It is energy-intensive, consuming approximately 50 kWh per kilogram of silicon produced. The carbon monoxide (CO) generated during the reaction is further oxidized to CO_2, resulting in modest emissions of less than 0.3 g CO_2 per kWh. Annually, over 7 million tons of MG-Si are produced, primarily for use in the steel and aluminum industries, with a market price of around 2–3 USD per kilogram.

Stage 2: Purification to Solar-Grade Silicon (SG-Si)

The second stage involves the purification of MG-Si to achieve solar-grade silicon (SG-Si), with impurity concentrations as low as 10^{-7} to 10^{-9}. This purification process is shared with the electronics industry and consists of the following steps:

1. **Hydrochlorination**: MG-Si, in powdered form, reacts with hydrochloric acid (HCl) in a fluidized bed reactor. This exothermic reaction produces trichlorosilane ($SiHCl_3$) and hydrogen (H_2):

$$Si + 3HCl \rightarrow SiHCl_3 + H_2.$$

2. **Distillation**: The trichlorosilane is purified through fractional distillation. Since $SiHCl_3$ is liquid at temperatures below 30°C, it is easily separated from gaseous impurities and hydrogen.

3. **Chemical Vapor Deposition (CVD)**: The purified trichlorosilane is then converted into high-purity polysilicon using the Siemens reactor. In a CVD reactor, trichlorosilane is decomposed at high temperatures (1100–1300°C) onto a U-shaped rod of pure silicon. This process consumes approximately 200 kWh per kilogram of silicon and takes about 10 days to produce one ton of polysilicon. The resulting polysilicon is broken into irregular fragments for further processing.

An alternative to the Siemens reactor is the production of granular silicon in a fluidized bed reactor. This method operates at lower temperatures (around 800°C) and involves the deposition of silicon onto seed particles, resulting in granular silicon suitable for solar applications.

Stage 3: Production of Monocrystalline Silicon

To produce monocrystalline silicon, the polysilicon obtained from the Siemens process or fluidized bed reactor is melted in a crucible. A seed crystal of monocrystalline silicon is dipped into the molten silicon and slowly rotated and pulled upward. This process, known as the **Czochralski method**, results in the growth of a single, large crystal of silicon. The cylindrical ingot produced is then sliced into thin wafers, which serve as the base material for high-efficiency solar cells.

Polycrystalline Silicon Modules

Polycrystalline cells are made by assembling multiple grains and plates of silicon crystals into thin wafers.

The manufacturing cost of this type of PV cells is less than that of monocrystalline silicon cells because smaller pieces of silicon are easier and less expansive to produce.

The polycrystalline cells are less efficient (from 16% to 18%), they have have a blue, speckled, and shiny appearance.

Polycrystalline cells are also very durable and may have a service life of more than 25 years.

The disadvantages of this type of PV technology are mechanical brittleness and a lower efficiency of conversion with respect to the mono-crystalline modules.

Thin-Film Technologies: Amorphous Silicon

Thin film photovoltaic cells are produced by depositing silicon film onto a substrate of glass.

This process allows the use of less silicon compared to mono- or polycrystalline cells, but this economy comes at the expense of conversion efficiency. Thin-film PV have efficiency encompassed between 6% and 10% for single crystal Si cells.

One effective strategy to boost the efficiency of solar cells is to design them with a layered, multi-cell structure.

This approach allows for better utilization of the solar spectrum, as each layer can be optimized to capture different wavelengths of light.

Among the various thin-film photovoltaic technologies, amorphous silicon stands out due to its versatility.

Unlike traditional silicon-based solar cells, amorphous silicon can be deposited onto a wide range of substrates, including flexible materials.

This opens up exciting possibilities for innovative applications, such as integrating solar cells into curved surfaces, wearable devices, or even building materials.

Another key advantage of amorphous silicon is its resilience to overheating. Traditional solar cells often suffer from performance degradation when temperatures rise, but amorphous silicon maintains its efficiency more effectively under such conditions.

This makes it a particularly attractive option for environments with high temperatures or intense sunlight. Over the years, amorphous silicon has emerged as one of the most widely developed thin-film PV technologies.

Thin-Film Technologies: Cadmium Telluride (CdTe)

Cadmium telluride (CdTe) photovoltaic technology is another promising type of thin-film solar cell that has gained significant attention in recent years.

They offer a lower cost per kilowatt-hour compared to many other solar technologies.

CdTe cells have achieved efficiencies in the range of 16% to 18%, making them a competitive option for large-scale solar installations.

A unique advantage of CdTe cells is their ability to capture shorter wavelengths of light more effectively than traditional silicon-based solar cells (that is the reason for its high efficiency).

This characteristic allows them to perform well in certain lighting conditions where silicon cells might struggle.

On the other end environmental concerns have been raised due to the potential toxicity of cadmium, particularly during the disposal or recycling of modules and the limited global supply of tellurium is still quiet limited.

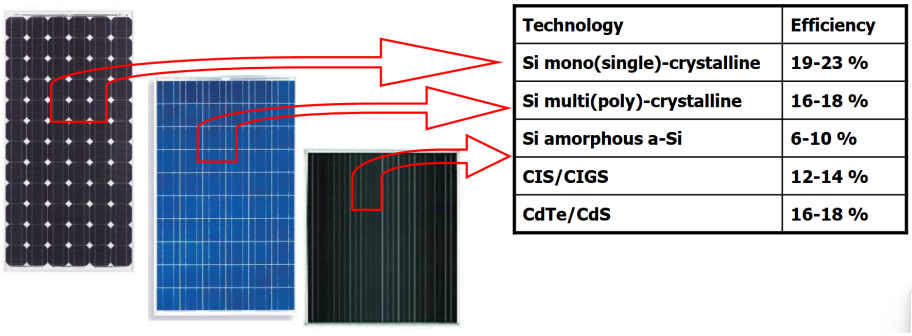

Technology	Efficiency
Si mono(single)-crystalline	19-23 %
Si multi(poly)-crystalline	16-18 %
Si amorphous a-Si	6-10 %
CIS/CIGS	12-14 %
CdTe/CdS	16-18 %

Figure 3: Shapes, colors and efficiency of different PV modules[3]

1.2 Solar Radiation and Site Selection

Solar radiation are electromagnetic waves emitted by the sun. This radiation is fundamental because without it there would be no life on Earth; moreover,

it allows the production of photovoltaic energy. This radiation is emitted by the sun in all directions, and a fraction of it arrives on Earth in three possible ways[3]:

- direct solar radiation: it penetrates the atmosphere and reaches the Earth's surface without dispersing at all on the way;
- diffuse solar radiation: it reaches the Earth's surface after having undergone multiple deviations in its trajectory, for instance by gases in the atmosphere;
- reflected solar radiation: it is reflected by the earth's surface itself, in a phenomenon known as the *Albedo effect*.

In reality, the parameters used for the sizing of PV are the global horizontal irradiation (GHI), which corresponds to the sum of direct and diffuse irradiation components received by a horizontal surface and is usually measured in kilowatt hours per square meter (kWh/m^2) and the global tilted irradiation (GTI) which corresponds to the sum of direct and diffuse irradiation components received by the tilted surfaces of the module[4].

The GHI allows us to compare the conditions for implementation of any PV technology without considering a particular technical design and mode of operation.

It must be considered that, in a given site, GHI is modified by air temperature, wind, snow, atmospheric pollution, dust, and some other geographical factors. GHI is a simplified approximation and does not fully describe the actual potential for PV power production. In the following two figures, the relation between GHI and specific photovoltaic output power[5] is shown:

Figure 4: Global horizontal irradiation (GHI) potential.

[3]Source: word bank
[4]Measured in kWh/m^2.
[5]Solar map

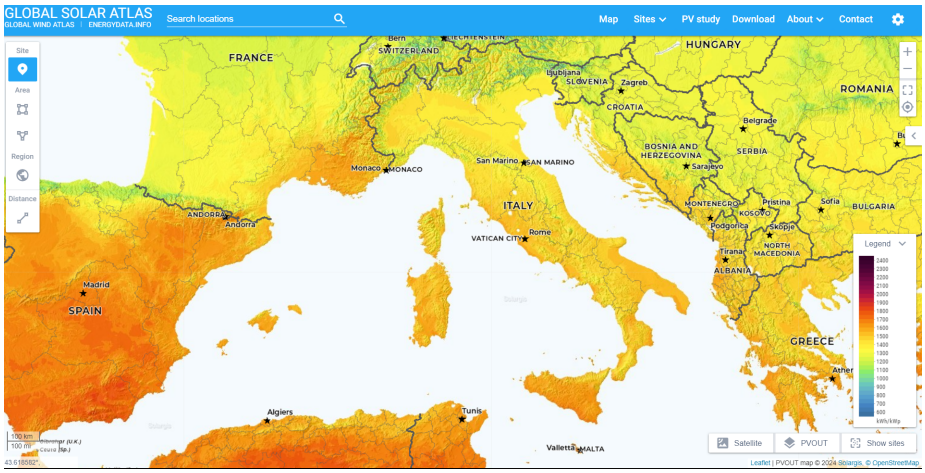

Figure 5: Specific photovoltaic power output.

As expected, the higher the GHI, the higher the specific photovoltaic power output [kWh/kWp], which is a metric that expresses the energy output that a module with a rated peak power of 1 kW can produce in one year. The relation is not purely linear because there are some disturbances.

Site Selection

As seen in Sec.1.2, the location in which the plant is built is very important for its energy production. The location of the plant is in Italy, in the Molise region near Termoli, more precisely in the locality of Guglionesi (41.895°N, 14.933°E), and its choice depends on different reasons:

- The GHI in the selected zone is the best you can get in Molise region according to:"GLOBAL SOLAR ATLAS"[6] and the yearly GTI measured with PVGIS is 1874 kWh/m^2.
- The wind, on average, blows at a speed of 3.1 m/s at 10 meters above the ground. The effect of the wind is beneficial as it improves the heat exchange between the modules and the air, helping to keep them cooler. If the module is at a temperature of 25 °C and under Standard Test Conditions (STC), it will produce its nominal power. However, as the temperature increases, the power output decreases.
- From a logistical point of view, this is a good compromise, as there is the port of Termoli that can manage the shipment via sea and a good road and highway network is present to facilitate truck transportation of all the needed equipment for the plant.

[6]Solar irradiation map

- The site is located in a sparsely populated area, so the prices for the land should not be very expansive;
- 'NYMBY' (not in my backyard) effect should not be a problem for the reason mentioned in the previous point;
- The DSO (distribution system operator) is in charge of deciding if the plant should be connected to the high voltage or the medium voltage grid; in both occurrences,the location is near to the infrastructure needed, as can be seen from TSO grid map[8].
- The Opening of Termoli Gigafactory, Italy's first battery production plant is a project conducted by the joint venture Automotive Cells Company (ACC), comprising Stellantis, Mercedes, and Total.

  Battery production is set to begin in 2026, with the output primarily targeting electric vehicles.

  Initial production is expected to reach about 60 million cells annually, with the potential for future expansion. The factory will have a production capacity of 40 GWh per year by 2028, and this facility will require significant energy and the solar plant could sell a part or its whole energy production with a bilateral contract to the Gigafactory.

Overview of Photovoltaic Plant Architecture

Before proceeding with the choice of topology, modules, inverters and transformers, a brief and simplified explanation of the whole system function of a Photovoltaic Plant is presented. In a photovoltaic system, the generators are the solar modules, which convert the sunlight directly into direct current through the *photovoltaic effect*1.1. These modules are usually arranged in series and/or parallel configurations to achieve the desired voltage and current levels.

The generated DC power is then transmitted via appropriately sized cables to the inverter. The inverter role is to convert the DC power into alternating power (AC), which is compatible with the grid or the local loads.

In many systems, especially those connected to a public grid, a transformer is used after the inverter: it steps up the voltage level from the inverter to match that required by the grid, and can also provide electrical isolation for additional safety.

Protection systems are an essential part of the overall design to ensure both equipment safety and human protection. Surge Protection Devices (SPDs) shield the system from transient overvoltages, such as those caused by lightning, switching events or electromagnetic disturbances. Switches and load break disconnectors allow for safe isolation of parts of the system during maintenance or in case of emergency; load break disconnectors, are designed to safely disconnect circuits that are under load. Fuses provide overcurrent protection by interrupting the circuit if the current exceeds safe limits, preventing potential damage or fire hazards.

Finally, all the cables within the system are selected and installed based on their ability to carry the necessary current while minimizing losses and ensuring compliance with safety standards. These cables link together the different components, modules, inverter, transformer and protection devices forming an integrated system that converts, conditions and safely distributes the electricity generated from solar energy.

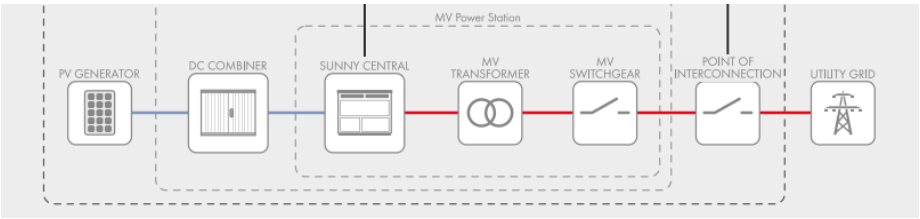

Figure 6: Main Components of a photovoltaic system [4].

1.3 Topology Optimization in Large-Scale PV Plants

The idea of this project is to realize a sort of "modular unit" with a rated power of about 2.5 MVA, integrating all the components necessary for power generation. The site considered is Guglionesi, but adapting the design logic with some minor changes the modular unit can be installed in other locations. The aim of an utility scale (or large scale) plant is to sell electrical energy either on the *Day-Ahead Market (DAM)* or*Long-Term Market (LTM)* and maximize the profits that come from these sales; in order to do so, scale economy is applied to cut the plant costs.

In Fig.7, it is possible to see that the weighted average total cost for kW installed, in the last 13 years, is dropped of the 85.7%, going from 5310 $/kW to 758 $/kW.

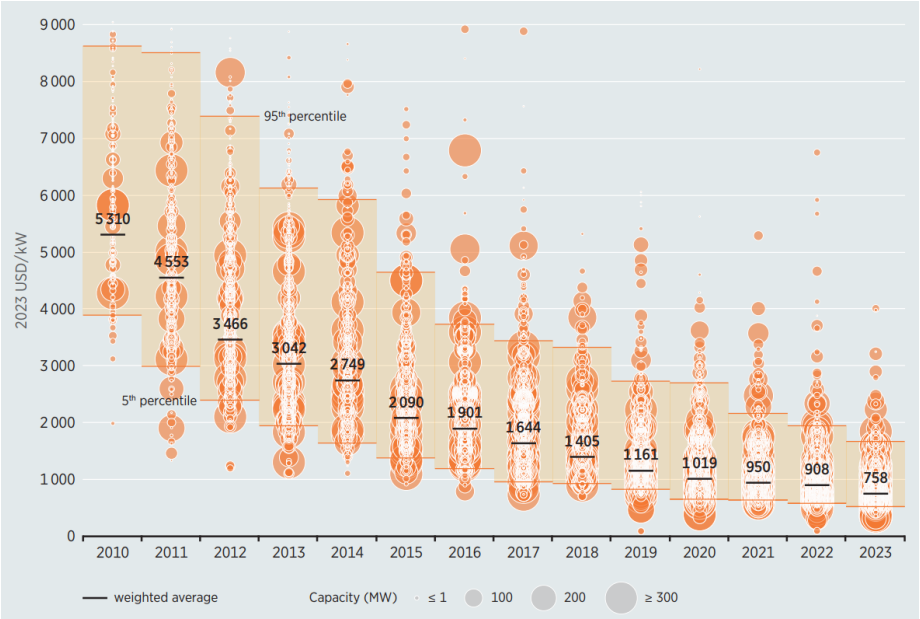

Figure 7: Total installed cost of utility-scale solar PV by project and weighted average for utility-scale systems, 2010-2023[5].

Topologies

There are three basic topologies for the plant:

1. string inverter;
2. multistring inverter;
3. central inverter.

String Inverter

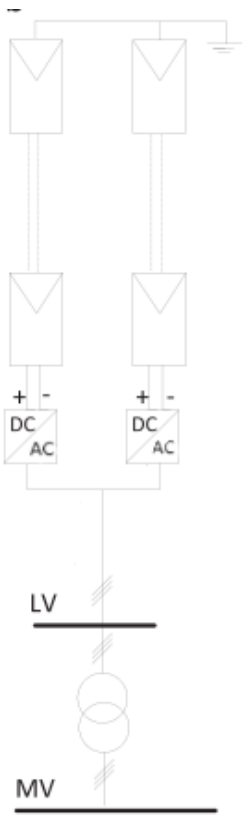

Figure 8: String inverter schematic.

In the string topology each string has its own inverter.

Table 2: Typical Parameters of string Inverters.

Topology	String inverter
Power (P) [kW]	0.06–0.4
Input Voltage ($\mathbf{Vin}_{DC}$) [V]	20–100
MPPT Voltage Range ($\mathbf{Vin}_{DC,MPPT}$) [V]	20–100
Output Voltage ($\mathbf{Vout}_{AC}$) [V]	110–230
Frequency (f) [Hz]	50, 60

Multi String Inverter

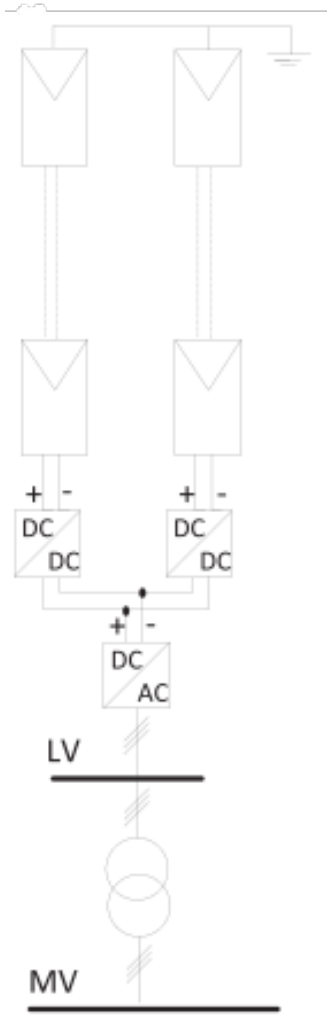

Figure 9: Multi string inverter schematic.

In multi string topology one string is connected to a DC/DC converter, then 4 or 5 DC/DC converters are connected to one inverter which may be close to the DC/DC converter or not depending on the layout of the plant.

Table 3: Typical Parameters of String and Multistring Inverters.

Topology	Multistring
Power (P) [kW]	2–30
Input Voltage ($\mathbf{Vin}_{DC}$) [V]	100–1000
MPPT Voltage Range ($\mathbf{Vin}_{DC,MPPT}$) [V]	200–800
Output Voltage ($\mathbf{Vout}_{AC}$) [V]	270–400
Frequency (f) [Hz]	50, 60

Centralized Inverter

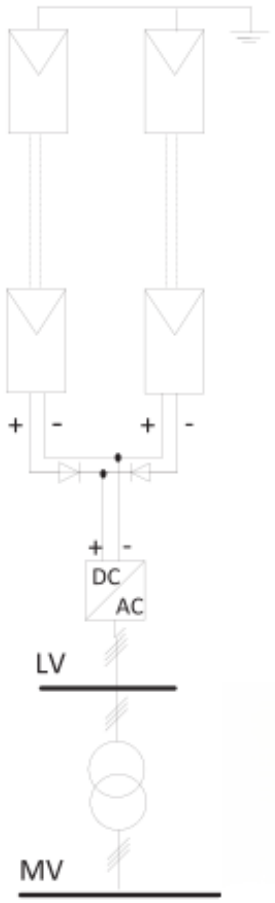

Figure 10: Central inverter schematic.

In the central inverter topology up to several thousands of modules are connected forming an array. The array is organized with string connected in par-

allel and the string is composed by module connected in series. Usually this topology uses a three winding transformer but since the proposed inverter will be 2.475 MVA rated the transformer BT/MT should be approximately 4.95 MVA rated. Such powerful transformer are usually made on demand and with customized characteristic, the absence of data for this kind of electrical machine led to the choice of a two winding transformer, having said that a three windings transformer is a valid option for this project.

Table 4: Typical Parameters of Central Inverters.

Topology	Central
Power (P) [kW]	100–4000
Input Voltage ($\mathbf{Vin}_{DC}$) [V]	400–1500
MPPT Voltage Range ($\mathbf{Vin}_{DC,MPPT}$) [V]	600–1200
Output Voltage ($\mathbf{Vout}_{AC}$) [V]	300–500
Frequency (f) [Hz]	50, 60

In an intersting paper wrote by A. Cabrera-Tobar et al.[6], some of the biggest utility scale plant (realized until 2016) where compared. Their work will be analyzed to choose the best topology for the case under study.

Some preliminary considerations can be made to help select the most suitable components for the system:

- The plants are developed by different companies: SMA, ABB, SunPower and Danfoss;
- the power of modules installed goes from 6 to 290 MW;
- the technology adopted are mainly m-Si and thin film.

in Tab.5 are showed their main characteristic:
Legend:
M = multi string inverter;
C = centralized inverter;
m-Si = mono-crystalline silicon modules;
c-Si = mono-crystalline and poly-crystalline modules used in the same plant.

Photovoltaic power plant	**Power (MWp)**	**Area (km^2)**	**modules ($\times 10^3$)**	**module type**	**Inverters number**	**Topology**
Korat I	6.0	0.13	29	m-Si	540	M
Rapale	7.7	0.49	100	Thin film	900	M
Airport, Athens	8.0	0.24	12	m-Si	12	C
Saint Amadou	8.5	0.24	113	Thin film	16	C
Volkswagen Chattanooga	9.5	0.13	33	m-Si	16	C
Masdar	10	0.22	87	m-Si, Thin film	16	C
Adelanto	10.4	0.46	46	m-Si	30	C
Taean	14	0.30	70	m-Si	28	C
Jacksonville	15	0.40	100	Thin film	23	C
San Antonio	16.0	0.53	214	m-Si	22	C
Cotton Center	18.0	0.58	93	m-Si	30	C
Almaraz	22.1	1.2	185	m-Si	6697	C
Veprek	35.1	0.83	185	m-Si	3069	C
Long Island	37.0	0.38	164	m-Si	30	C
Reckahn	37.8	0.98	487	Thin film	43	C
Ban Pa-In	44.0	0.8	900	Thin film	84	C
Lieberose	71.0	2.2	900	Thin Film	38	M
Kalkbut	75.0	2.3	312	m-Si	124	C
Eggebek	80.0	1.2	76	m-Si	3200	M
Montalto di Castro	85.0	2.83	280	c-Si	124	C
Templin	128.0	2.14	1500	Thin Film	114	C
California Valley Ranch	250	6.01	749	c-Si	400	C
Agua Caliente	290	9.71	5200	Thin Film	400	C

Table 5: Large Scale Photovoltaic Power Plants[6].

The first choice is about the modules technology, m-Si are more expansive than Thin film, but, on the other end they can provide an higher efficiency that result in less land consumption and a lower length of cables needed to for the same installed power, for this reasons m-Si modules will be implemented.

One thing that can be noticed is that there is not even one singular string inverter topology, this is due to the fact that this technology would cause higher cost for: the huge number of inverter needed, their maintenance and a very complex system of cables to transport the energy to the step up transformer. The remaining topology are central inverter and multistring inverter.

The central inverter (at least in this analysis) seems to be the most used, this comes from the fact that for such a number of modules the central inverter represents the best solution from a strictly practical point of view since it requires a lower number of cables and less maintenance, moreover economically speaking the central inverter topology could lead to a lower overall cost compared to multistring inverter.

Typically, a higher installed power capacity leads to a reduction in the total installed cost per kilowatt, but the problem, especially for the Italian situation, is that the low voltage/medium voltage substation (LV/MV substation), medium voltage/high voltage substation (MV/HV substation) and the power transmission lines are almost always at the limit of their capacity, thus adding a very large plant (e.g. 30 MW) would involve expanding the electrical infrastructure in the area by increasing the total installation costs. From this consideration modular unit of about 2.5 MW has been chosen since gives a certain margin of flexibility to install plants in a lot of different locations. For this project, 4 of this units will be installed in the same site.

Tab.6 and Fig.11 summarize the characteristics of the topologies presented before(plus module integrated topology):

Table 6: Main characteristics of PV inverter topologies[6]

Characteristics		**Central**	**String**	**Multistring**	**Module integrated**
Performance	Reliability	L	H	M	H–H
	Robustness	H	L	M	L–L
	Flexibility	L	H	M	H–H
	MPPT efficiency	L	H	M	H–H
Power losses	Mismatching	H	L	L	L–L
	Switching	H	L	M	L–L
	AC power losses	L	M	M	H
	DC power losses	H	L	M	L–L
	AC voltage variation	L	H	M	H–H
Power quality	DC voltage variation	H–H	M	H	L–L
	Voltage balance	H	M	L	L
Cost	Installation cost	M	H	M	H–H
	DC cables	H	L	M	L–L
	AC cables	H	M	M	H
	Maintenance	L	M	H	H–H

The following nomenclature is used: H–H: very high, H: High, M: Medium, L: Low, L–L: very low.

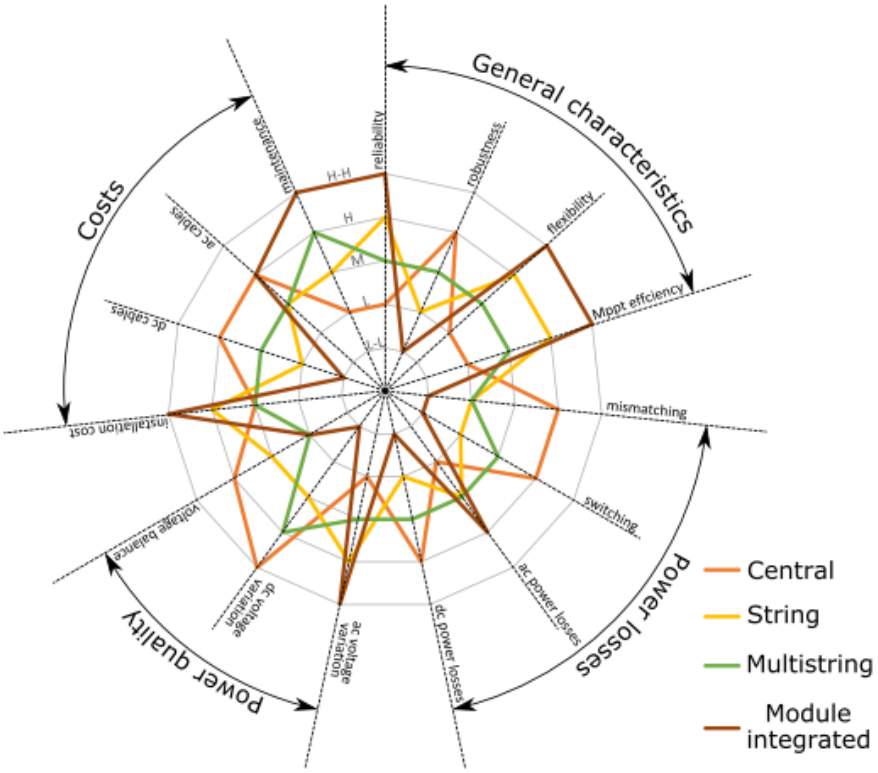

Figure 11: Comparison between different PV inverter topologies characteristics for utility scale systems [6].

The topologies compared include central, multistring, and an additional topology known as the multicentral inverter.

The multicentral inverter topology integrates several central inverters, each with a power rating of less than 100 kW, into a single cabinet. Within this cabinet, there are three ore more PV inverters with identical characteristics. Each inverter operates with its own individual MPPT (Maximum Power Point Tracking) control, ensuring optimal management of the connected PV strings. The outputs of these inverters are connected in parallel, equipped with appropriate protection mechanisms, to provide a single consolidated output for the entire cabinet.

In Fig.12 there is a comparison between three different topologies in terms of: cost/power, efficiency and power/area.

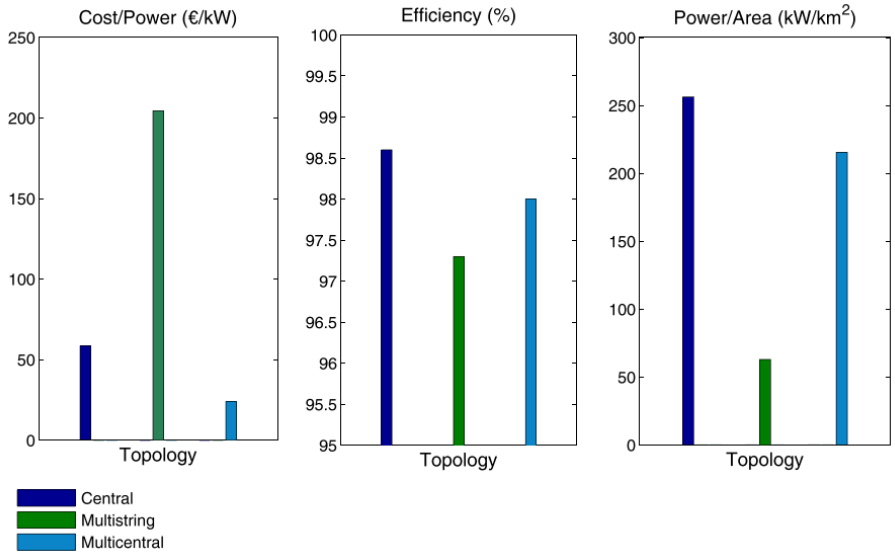

Figure 12: Comparison between different PV inverter topologies available in the market for utility scale PV system[6]

Choosing the optimal topology is not an exact science and depends on different variables. Although the analysis suggests that the theoretically best topology is the multi-central inverter solution (excluding land consumption), evaluating the MWp/Inverter ratio in Fig.7 reveals that, except for the last five sites, which follow a multi-inverter topology, all other sites should adopt a central inverter topology. This conclusion is derived from the installed power per single inverter.

plant name	MWp	N° inverter	MWp/inverter
Lieberose	71.0	38	1.87
Templin	128.0	114	1.12
Volkswagen Chattanooga	9.5	10	0.95
Reckahn	37.8	43	0.88
Kalkbut	75.0	84	0.89
Adelanto	10.4	13	0.80
Jacksonville	15.0	20	0.75
Long Island	37.0	50	0.74
San Antonio	16.0	22	0.727
Agua Caliente	290.0	400	0.725
Ban Pa-In	44.0	61	0.72
Montalto di Castro	85.0	124	0.685
Airport, Athens	8.1	12	0.675
Masdar	10.0	16	0.625
California Valley Ranch	250.0	500	0.5
Taean	14.0	28	0.5
Cotton Center	18.0	36	0.5
Rapale	7.0	900	0.0086
Veprek	35.1	3069	0.011
Korat I	6.0	540	0.011
Eggebek	48.0	3200	0.015
Almaraz	22.1	6697	0.0033

Table 7: MWp/Inverter ratio.

The final guideline for the project are summarized in Tab.8:

module type	m-Si
Topology	central inverter
Inverter number	4
P_{AC} output [MVAR]	9.5-10.5
Transformer type	two winding BT/MT

Table 8: Plant guidelines.

1.4 Photovoltaic Module Choice and Modeling

The module chosen is the LR7-72HGD 620M from LONGi[7] that is the global leader company in Photovoltaic modules production. The model is a monocrystalline silicon module designed for utility scale project, its main advantages are:

- high efficiency (up to 23%), the efficiency is improved by the fact that the module has 80 % bifaciality, that means also the back part of the module

[7]LONGi website.

is capable of generating energy (more precisely it can generate the 80% of the enegy generated from the frontal side given the same irradiance);

- the module is formed by 2 strings of cells in parallel, each string has 72 cells in series. Three bypass diode protect the module. In normal conditions every cell generate current in an uniform way and the bypass diodes stay inactive, but when there is a partial shading the bypass diode become active avoiding that current flows in the shade part of the module over-heating it. In this way the remaining part keep producing energy;
- the variability of the sort circuit current, open circuit voltage and maximum power output with the temperature is one of the main problems of PV modules. The coefficient of variability of the selected module are elite, actually they are almost half of other competitor models on the market;
- the producer offer a 12 years warranty on the product and a 25 years warranty on power output, the power output trend is showed in Fig.13. The producer guarantees a first year power degradation lower than 1%, a yearly power degradation of 0.4% from year 2 to year 30 and in any case at least 84.8% power output after 25 years.

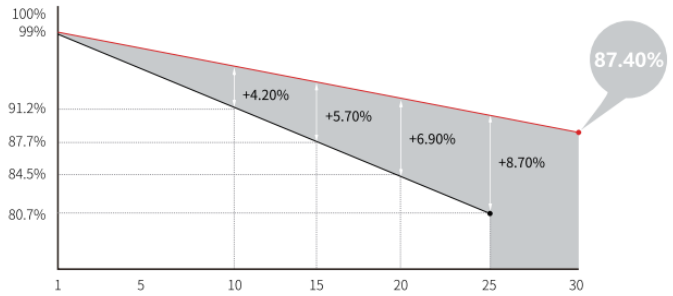

Figure 13: Module's performance degradation due to aging.

Manufacturer	LONGi
Model	LR7-72HGD 620M
Country	China
Cell type	Mono-Cristalline
No. of cells	144 (6x24)
Dimensions [mm]	2382x1134x30
Weight [kg]	33.5
Maximum Power [W]	620 (STC condition)
P_{max} uncertainty	$\pm$ 3%

Table 9: General information about the module.

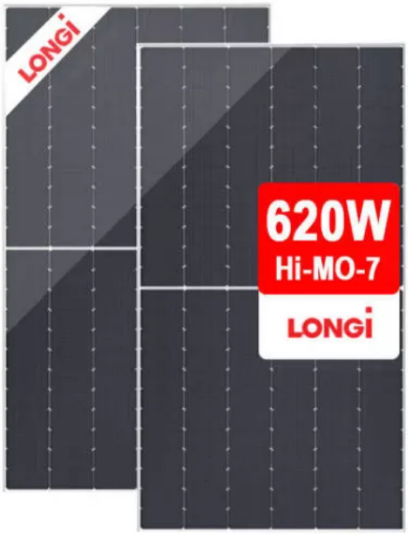

Figure 14: LR7-72HGD 620M module picture.

Manufacturer	LONGi
Model	LR7-72HGD 620M
Maximum power voltage [Vmp]	44.55
Maximum power current [Imp]	13.92
Open-circuit voltage [Voc]	52.66
Short-circuit current [Isc]	14.81
Module efficiency STC [%]	23
Operating temperature range [°C]	-40°C to +85°C
Maximum system voltage [V]	DC 1500
Maximum series fuse rating [A]	30
Power tolerance [%]	3
$\gamma_{\mathbf{Pm}}$ **(Temperature coefficients of Pmax) [%/°C]**	-0.28
$\beta_{\mathbf{Uoc}}$**(Temperature coefficients of Voc) [%/°C]**	-0.23
$\alpha_{\mathbf{Isc}}$**Temperature coefficients of Isc [%/°C]**	+0.045
Protection Class	II
Nominal operating cell temperature (NOCT) [°C]	45 ± 2
Price [\EUR]	130 (stimato)

Table 10: Module reference value: STC= AM 1.5 1000 W/m^2 25°C; NOCT= AM 1.5 800 W/m^2 20°C 1m/s.

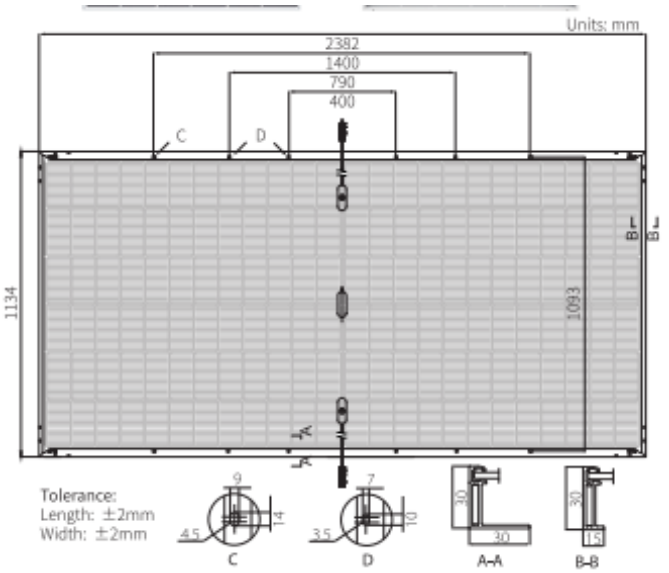

Figure 15: Dimensions of the Module in mm.

For module mounting operations LONGi offers an Installation Manual for Solar PV Modules[15] that give a lot of guidelines. The final mounting operations will be realized taking into account the installer experience and asking the advice of the producer of the modules.

1.4.1 V-I Characteristic Curve Reconstruction

The producer of the module gives in the data-sheet only 4 points of the V-I characteristic: I_{sc}, V_{oc}, V_{mpp} and I_{mpp}.

Over the years, a lot of different models have been proposed in the literature to build the PV characteristic curves starting from the data that are given from the manufacturer. Based on their derivation, Photovoltaic models can be classified into three main categories: circuit-based, analytical-based, and empirical-based models.

The model proposed is an analytical based model proposed for the first time in [16] and made more popular in [17] and [18]. It is a two-parameter model that requires only two fitting parameters:

$$C_1 = \left(1 - \frac{I_{mpp}}{I_{sc}}\right) \cdot \exp\left(-\frac{V_{mpp}}{C_2 V_{oc}}\right) = \frac{I_{sc}}{1 - \exp\left(-\frac{V_{oc}}{C_2}\right)} \tag{1}$$

$$C_2 = \frac{V_{mpp} - V_{oc}}{\ln\left(1 - \frac{I_{mpp}}{I_{sc}}\right)} \tag{2}$$

Using this two parameter the current of the photovoltaic module is obtained with Eq.(3):

$$i_{pv} = I_{sc} - C_1 \exp\left(-\frac{V_{oc}}{C_2}\right)\left(\exp\left(\frac{v_{pv}}{C_2}\right) - 1\right) \tag{3}$$

The result in Fig.16 is obtained with the "MATLAB" code in appendixA.

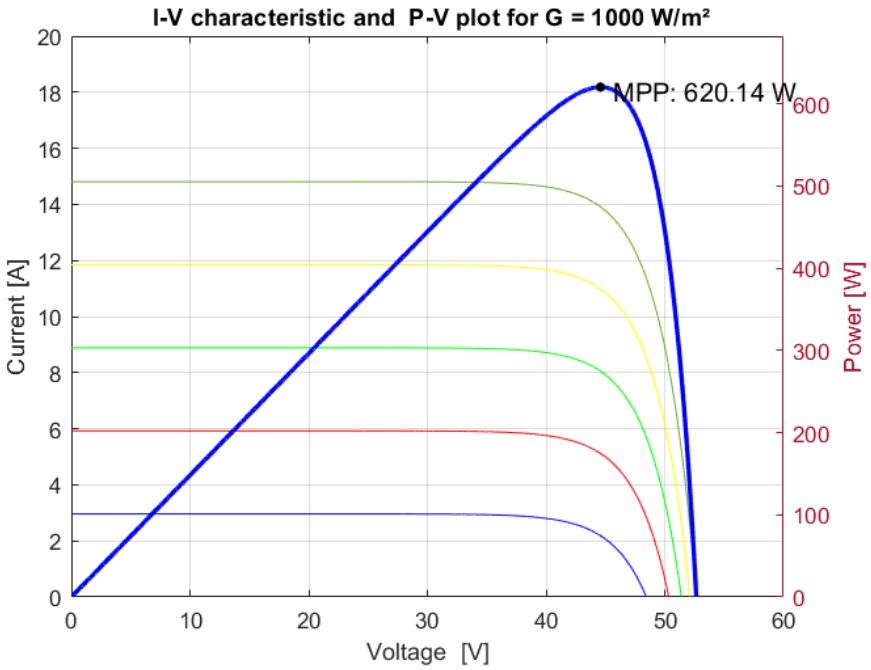

Figure 16: Module's V-I Characteristic and MPP.

The model adopted is been chosen after analyzing the comparative paper [19] in which the three main kinds of models are presented with their advantages and disadvantage, this model is a good compromise between simplicity and accuracy, The error on the Maximum Power Point value is only about 0.02%, way below the IEC EN 50530 standard suggestions that impose an absolute errors within the vicinity of MPP lower or equal to 1%.

1.5 Inverter for Grid-Connected PV Systems

The inverter selected is the "SMA Sunny central 2475 kVA", it is a solution designed for utility scale projects, its main advantages are:

- high efficiency, up to 98.6% at 35°C with a gradual derating for higher temperatures;

- European efficiency 98.4%[8] that shows that the inverter has a good efficiency also with low loads;
- high protection rating IP 65 gives the possibility to install it outdoor;
- Opticool cooling system, it is a smart system that can dynamically adapt to external conditions and allows operation up to exterior temperature of 60°C;
- up to 4 inverters transportable in a standard container.

Figure 17: Inverter picture and information[4].

[8] $\eta_{\mathrm{EU}} = 0.03 \cdot \eta_{5\%} + 0.06 \cdot \eta_{10\%} + 0.13 \cdot \eta_{20\%} + 0.10 \cdot \eta_{30\%} + 0.48 \cdot \eta_{50\%} + 0.20 \cdot \eta_{100\%}$

Manufacturer	SMA
Model	Sunny central 2475
Input (DC)	
MPP voltage range V_{DC} (at 25°C/ 35°C / at 50°C)	638 V to 950 V/ 800 V/ 800 V
Max. input voltage V_{DC}	1100 V
Max. input current I_{DC}, max (at 35°C/ 50°C)	3960 A / 3600 A
Number of DC inputs	24 double pole fused (32 single pole fused)
Max. number of DC cables per DC input (for each polarity)	2 x 800 kcmil, 2 x 400 mm^2
Available DC fuses sizes (per input)	200 A, 250 A, 315 A, 350 A, 400 A, 450 A, 500 A
Output (AC)	
Nominal AC power at $\cos \varphi = 1$ (at 35°C / 50°C)	2475 kVA/ 2250 kVA
Nominal AC power at $\cos \varphi = 0.8$ (at 35°C / 50°C)	1980 kW / 1800 kW
Max. output current $I_{AC,max}$= Nominal AC current $I_{AC,nom}$	3300 A
Max. total harmonic distortion	<3% at nominal power
Nominal AC voltage/ nominal AC voltage range	434 V / 347 V to 521 V
AC power frequency / range	>2
Power factor at rated power/ displacement power factor adjustable	1 / 0.8 overexcited to 0.8 underexcited 1 / 0.0 overexcited to 0.0 underexcited
Efficiency	
Max. efficiency/ European efficiency/ CEC efficiency	98.6%/ 98.4%/ 98%

Protective Devices	
Input-side disconnection point	DC load break switch
Output-side disconnection point	AC circuit breaker
DC overvoltage protection	Surge arrester, type 1
Degree of protection (IEC 60529): electronics / air duct / connection area	IP65 / IP34 / IP34
General Data	
Dimensions (W/ H / D)	2780 / 2318 / 1588 mm
Weight	<3400 kg
Max. self-consumption (operation)/ self-consumption (stanby)	<2000 W / <300 W
Internal auxiliary power supply	integrated 8.4 kVA transformer
Operating temperature range	-25°C to 60 °C
Temperature range (standby)	-40°C to 60°C
Temperature range (storage)	-40°C to 70°C
Max. permissible value for relative humidity (condensation)	0% to 95%
Maximum operating altitude above MSL	1000 m
Fresh air consumption	6500 m^3/h

Features	
DC connection	Terminal lug on each input (without fuse)
AC connection	With busbar system (three busbars, one per line conductor)
Communication	Ethernet, Modbus Master, Modbus Slave
Communication with SMA string monitor	Modbus TCP / Ethernet (FO MM, Cat-5)
Enclosure / roof color	RAL 9016 / RAL 7004
Supply transformer for external loads	2.5 kVA
Certificates and approvals	CE, IEC / EN 62109-1 , IEC / EN 62109-2, VDE AR-N 4110/4120, IEEE1547,UL 840 Cat. IV, Arreté du 23/04/08
EMC standards	IEC / EN 61000-6-2, FCC Part 15 Class A, Cispr 11, DIN EN55011:2017

1.6 Power Transformers

The chosen transformer is a "Trihal" - Cast Resin Transformer [9] from the Schneider electric. Its main features are:

- it is designed to reduce load and no load losses;

[9] Trihal 20 kV transformer.

- the cast resin windings require less maintenance that reduce the costs in the long run, but still ensure a long operative life of the machine;
- protection rating IP 31;
- can be integrated with SCADA system for gathering and analyzing of data.

In Fig.18 are represented the dimensions of the transformer:

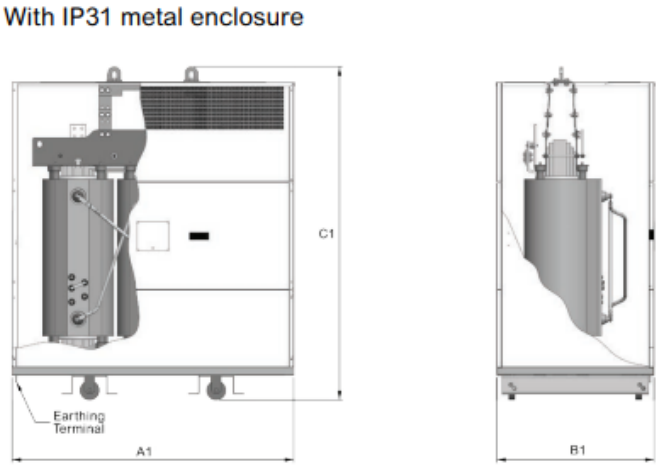

Figure 18: Transformer dimensions.

A1 [mm]	2340
B1 [mm]	1280
C1 [mm]	2700
Weight enclosure [kg]	270
Total weight [kg]	5200

The main parameter of the transformer are prented in Tab.11:

Parameter	Value
Power [kVA]	2500
Primary voltage [V]	400
Seconadry voltage [kV]	20
Insulation level HV [kV]	24
Tapping range HV	+/- 2.5% e/o +/- 5%
Vector Group	Dyn 11
No load losses [W]	2790
Load losses at 120 °C (W)	19000
Impedance voltage [%]	6
Acoustic level LWA [dB(A)]	70
Acoustic level LPA at 1m [dB(A)]	55

Table 11: Parameters of the 2500 kVA transformer.

2 System Sizing and Energy Yield Estimation

In this section, the sizing of the plant will be made following the procedure proposed by SMA in its manual "Planning of a PV Generator"[20].

The following steps outline the necessary calculations when designing a PV plant. The recommended procedure is the following:

- **Calculate the power dimensions of the PV plant**
  - Determine the AC active power (P_{AC}) and the DC input power (P_{DC}) of the inverter.
  - Define the nominal power ratio.
- **Calculate the voltage dimensions**
  - Calculate the voltage dimensions at the PV module level.
  - Calculate the voltage dimensions at the string level.

AC Power Determination of the Inverter

The first step is to determine the amount of active power injected into the connection point with the electrical grid; this value can be easily found considering the apparent power of the inverter S_{AC} (2475 kVA) and the power factor cos φ using the Eq.4:

$$P_{AC} = S_{AC} \cdot cos\varphi \tag{4}$$

Where:
P_{AC} = AC active power;
S_{AC} = Apparent power of the inverter;
cos φ = Power factor.
Considering cos $\varphi = 1$ we obtain:

$$P_{AC}=2475 \text{ kVA} \cdot 1 = 2475 \text{ kW}$$

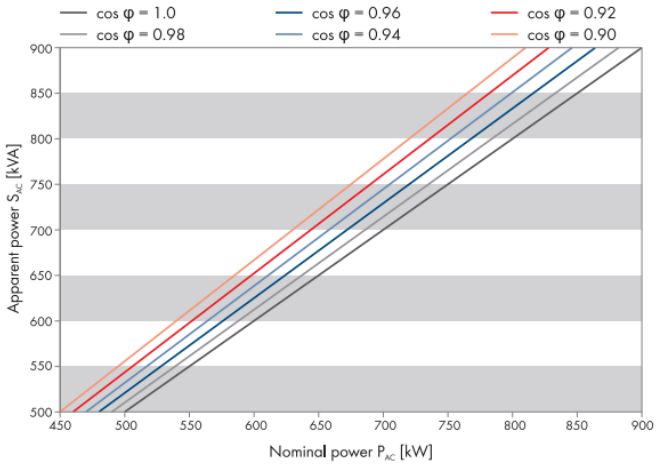

Figure 19: Dependence of AC Active Power on the Power Factor (cos φ).

DC Power Determination of the Inverter

Dividing the DC input power by the inverter efficiency, is possible to calculate the DC input power required to achieve the desired AC active power that will be fed into the grid.

Also, it is necessary to mention that the efficiency of the inverter depends on the PV array voltage, decreasing with high input voltages.

This input power can be found by using the following Eq.5:

$$P_{DC} = \frac{P_{AC}}{\eta} \tag{5}$$

Where:
P_{DC} = DC input power of inverter;
P_{AC} = AC active power of inverter;
η = Inverter efficiency.

The maximum efficiency measured for the inverter selected is 98.6%, this value will be used.

$$P_{DC}=\frac{2475kW}{0.986} = 2510.14 \text{ kW}$$

Nominal Power Ratio

This ratio defines the ratio between the DC power of the inverter and the DC power of the PV array. It is used beacuse it is crucial to avoid oversizing the

inverter, as its efficiency peaks when it works at nominal power and diminishes when the power is significantly lower than its nominal capacity.

NPR is calculated as:

$$NPR = \frac{P_{DC}}{P_{DC,array}} \tag{6}$$

Where:
NPR = Nominal power ratio;
P_{DC} = DC power of the inverter;
$P_{DC,array}$ = PV array power.

$$\text{NPR}=\frac{2510kW}{2650kW} \approx 0{,}947$$

In a photovoltaic system, the DC power of solar modules installed is generally greater than the DC power of the inverter. This is done to maximize energy production and to optimize the performance of the system.

The main reasons to perform this oversizing operation are the following:

- Solar modules rarely operate at their maximum nominal power due to various factors, such as weather conditions, angle of sunlight incidence, temperature, dust and other losses. Oversizing the photovoltaic field allows for better utilization of the inverter even under suboptimal conditions;
- Inverters tend to operate more efficiently when they are close to their maximum capacity. By oversizing the DC power of the modules, it is possible to ensure that the inverter runs at high power levels for longer periods during the day, thereby improving the overall efficiency of the system;
- Oversizing the photovoltaic field compared to the input power of the inverter is often more cost-effective. This approach allows for an increase in energy production without significantly raising the cost of the inverter, which is a costly component;
- The exceeding cost due to curtailment of energy and cost of extra modules is partially compensated by the decrease of the capture rate effect

Capture Rate

Capture rate is a phenomenon that is emerging in electrical grids with high penetration of solar capacity installed. It consists in the fact that given the abundance of energy at very low prices (often in the pay as clear markets the solar and wind farm offer their energy with prices near to zero) the price of electricity drops in the central hours of the day.

In Fig.20 is showed the normalized price of energy in the Italian energy market at each hour of the day in the 2024:

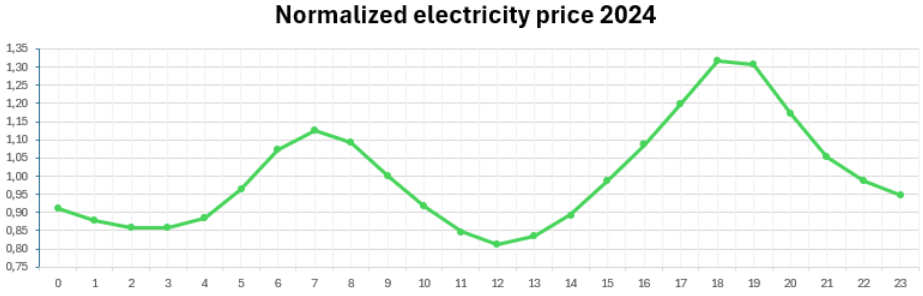

Figure 20

The price is normalized considering 108.51 €/MWh, it is easy to see that boosting energy production before 10 AM or after 2 PM is economically convenient.

2.1 Voltage Ratings and Electrical Constraints

The temperature modifies the electrical performance of the photovoltaic modules: in particular, the performance deteriorate with the increasing of the temperature. The voltage is affected by this parameter more than the current, as it can be seen in the Fig.21; for this reason, the module voltage and the string current must be calculated considering the climate data of the location selected for the plant.

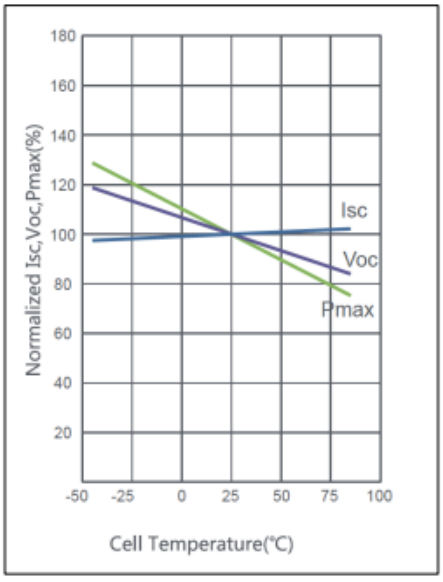

Figure 21: V_{oc} I_{sc} P_{max} temperature variation.

Maximum Open-Circuit Voltage

The open-circuit voltage is the highest at low temperatures. The maximum open-circuit voltage can be calculated using the open-circuit voltage and the temperature coefficient. The lowest temperature that can be expected at the mounting location must be taken into account, as showed in Eq.7

$$V_{DCmaxMOD} = V_{oc,STC}(1 + \beta \cdot (T_{min} - T_{STC})) \tag{7}$$

Where:

- $V_{DCmaxMOD}$: Maximum PV module voltage;
- $V_{oc,STC}$: Open-circuit voltage of PV module in standard conditions;
- T_{min}: Temperature coefficient at minimum expected temperature;
- T_{STC}: Temperature at standard conditions;
- β Temperature coefficient of V_{OC}.

Data on the minimum temperature were obtained comparing the result from three different sources: NASA Power Access Data Viewer [21] analyzing the minimum temperature from 1st january 2001 to 31th december 2022, 3B meteo archive[22] for the same timespan, and PVGIS[23] data from January 1st 2005 to December 31st 2023.

The first set of data showed a minimum temperature of about -0.6 °C.

The second one showed a minimum temperature of about -2.5 °C with a distribution showed in Fig.22 in which is shown in a graphical way the data set from NASA in which there are the trends of minimum, average and maximum temperature in the last 20 years.

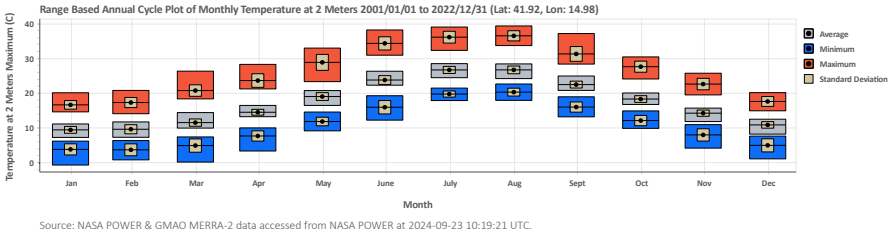

Figure 22: Minimum, average and maximum temperature in the last 20 years.

The third source PVGIS shows a minimum temperature of about -6°C that will be choosen for the calculation since is the worst case and since the data are showed hour by hour.

$$V_{DCmaxMOD} = 52.66 \text{ V} \cdot (1 + -0.23\%/°C \cdot (-6°C - 25°C)) = 56.41 \text{ V}$$

Minimum Maximum Power Point (MPP) Voltage

The open-circuit voltage is lowest at high temperatures. The minimum PV module voltage can be calculated using the open-circuit voltage and the temperature coefficient. The highest temperature that can be expected at the mounting location must be taken into account. To calculate $V_{DCminMOD}$ is used Eq.8:

$$V_{DCminMOD} = V_{mpp}(1 + \beta \cdot (T_{max} - T_{STC})) \tag{8}$$

Where:

- $V_{DCminMOD}$: Minimum PV module voltage;
- V_{mpp}: Voltage of the PV module at maximum power;
- T_{max}: maximum expected temperature;
- T_{STC} temperature in standard conditions;
- β Temperature coefficient of V_{OC}.

$$V_{DCminMOD} = 44.55V \cdot (1 - 0.23\%/°C \cdot (75°C - 25°C) \approx 39.4 \text{ V}$$

2.2 Solar Array Configuration

Maximum Module Current

Despite the fact that current is less dependent than voltage from the temperature, it still need to be calculated with the maximum operating temperature that the photovoltaic module can reach (75°C) whit Eq.9:

$$I_{DCmaxSTR} = I_{DCscMOD} = I_{SC} \cdot (1 + \alpha(T_{MAX} - T_{STC})) \tag{9}$$

Where:

- $I_{DCmaxSTR}$: Maximum string current;
- $I_{DCscMOD}$: Maximum module current;
- I_{SC}: Short-circuit current of the PV module;
- T_{max}: maximum expected temperature;
- T_{STC}:temperature in standard conditions;
- α temperature coefficient of I_{SC}.

One interesting thing to notice is that, unlike module voltage, the module current slightly increases as temperature rises. This happens because at higher temperatures, the silicon PN junction requires less energy to allow electron flow. In other words, for the same irradiance, a solar module can produce a slightly higher current at higher temperatures. However, since the voltage decreases more significantly, the overall power output of the module is reduced as temperature increases.

$$\mathrm{I}_{DCmaxSTR} = 14.81\ \mathrm{A} \cdot (1{+}0.045\% \cdot (75°C - 25°\mathrm{C}) \approx 15.14\ \mathrm{A}$$

In the following table shows the results obtained for the voltage dimensions of the PV plant:

Maximum Open circuit voltage [V]	56.41
Minimum MPP Voltage [V]	39.4
Maximum PV Module Current [A]	15.14

String Sizing: Minimum and Maximum Modules per String

A string must be composed by a certain number of PV modules which ensures that the string voltage is always below the maximum input voltage of the inverter. If the string voltage exceeds the input voltage of the inverter, yield losses can occur due to delayed starting or to damage to the inverter by overvoltage.

With Eq.10 the maximum number of PV modules in series per string is determined:

$$n_{maxMODSTR} \leq \frac{V_{DCmaxINV}}{V_{DCmaxMOD}} \tag{10}$$

Where:

- $\mathrm{n}_{maxMODSTR}$: Maximum number of PV modules per string;
- $\mathrm{V}_{DCmaxINV}$: Maximum input voltage of inverter;
- $\mathrm{V}_{DCmaxMOD}$: Maximum PV module voltage.

$$\mathrm{n}_{maxMODSTR} \leq \frac{1100V}{56.41} = 19.5 \approx 19 \text{ modules}$$

To avoid that the input voltage of the inverter goes below the minimum voltage of MPP tracking, it is also necessary to maintain the string voltage above de minimum MPP voltage of the inverter.

$$n_{minMODSTR} \geq \frac{V_{DCmppminINV}}{V_{DCminMOD}} \tag{11}$$

Where:

- $\mathrm{n}_{minMODSTR}$: Minimum number of PV modules per string;
- $\mathrm{V}_{DCmppminINV}$: Minimum MPP voltage of the inverter;
- $\mathrm{V}_{DCminMOD}$: Minimum PV module voltage.

$$\mathrm{n}_{minMODSTR} \geq \frac{638V}{39.4V} = 16.19 \text{ modules} \approx 17$$

Considering the calculations made before, the string of PV modules must follow the Eq.12:

$$n_{minSTR} \leq n_{STR} \leq n_{maxSTR} \tag{12}$$

In the case under study $17 \leq n_{STR} \leq 19$, in order to maximize the inverter's potential n_{STR} is chosen equal to 19.

Once the number of modules per string has been decided, the maximum and minimum string voltage can be calculated using Eq.13 and Eq.14:

$$V_{DCmaxSTR} = n_{MODSTR} \cdot V_{DCmaxMOD} \tag{13}$$

$$V_{DCminSTR} = n_{MODSTR} \cdot V_{DCminMOD} \tag{14}$$

Where:

- $V_{DCmaxSTR}$: Maximum string voltage;
- $V_{DCminSTR}$: Minimum string voltage;
- n_{MODSTR}: Number of modules per string;
- $V_{DCmaxMOD}$: Maximum PV module Voltage;
- $V_{DCminMOD}$: Minimum PV module Voltage.

These values must stay in the MPP voltage range of the inverter, between 638 V and 1100 V.

$$V_{DCmaxSTR} = 19 \cdot 56.41 \text{ V} = 1071.8 \text{ V}$$
$$V_{DCminSTR} = 19 \cdot 39.4 \text{ V} = 748.6 \text{ V}$$

It is possible to say that the limits previously mentioned are respected.

Optimal Number of Strings per Inverter

The input current of the inverter determine the maximum number of strings, while the minimum number of strings depend on the PV array power. With Eq.15 and Eq.16 is possible to calculate their values:

$$n_{maxSTR} = \frac{I_{DCINV}}{I_{DCmaxSTR}} \tag{15}$$

$$n_{minSTR} = \frac{P_{DCGEN}}{P_{maxMOD} \cdot n_{MODSTR}} \tag{16}$$

Where:

- n_{maxSTR}: Maximum number of strings;
- n_{minSTR}: Minimum number of strings;

- n_{MODSTR}: Number of modules per string;
- P_{DCGEN}: PV array power;
- P_{maxMOD}: Maximum PV module power;
- I_{DCINV}: Maximum input current of the inverter;
- $I_{DCmaxSTR}$ Maximum string current.

$$n_{maxSTR} \leq \frac{3960A}{15.14A} = 261.55 \text{ strings} \approx 261 \text{ strings}$$

$$n_{minSTR} \geq \frac{2650KW}{0.62kW \cdot 19} = 224.96 \approx 225 \text{ strings}$$

$$n_{minSTR} \leq n_{STR} \leq n_{maxSTR}$$

that from the previous operations results in:

$$225 \leq n_{STR} \leq 261$$

In Tab.12 there are the most important results obtained until this point:

PV module model	**LR7-72HGD 620M**
Maximum number of PV modules per String	19.5
Minimum number of PV modules per String	16.19
Number of PV Modules per String	**19**
Maximum string voltage	1071.8 V
Minimum string voltage	748.6 V
Minimum number of strings	224.96
Maximum number of strings	261.55
Number of strings per inverter	**260**

Table 12: Overview table of array sizing calculations.

After the sizing previously made for one inverter, it has been decided to use 4 centralized inverters for a nominal power of the PV plant output of about 9.9 MVA.

To find the number of total modules adopted in this configuration, Eq.17 is used:

$$n_{modules} = n_{MODSTR} \cdot n_{STR} \cdot n_{INV} \tag{17}$$

$$n_{modules} = 19 \cdot 260 \cdot 4 = 19760$$

2.3 Annual Energy Yield Prediction Using Performance Ratio (PR)

When designing a grid-connected PV system, it is important to estimate, as correctly as possible, the annual energy injected in the AC grid that is called: "yield of the system". These formulas can be used to calculate it:

$$E_{AC} = H_g \cdot S_{PV} \cdot \eta_{STC} \cdot PR \tag{18}$$

$$E_{AC} = P_N \cdot h_{eq} \cdot PR \tag{19}$$

Where:

- H_g: Annual irradiance on the modules mounted with the optimal angle $[\frac{kWh}{m^2}]$;
- S_{PV}: Total surface of the photovoltaic generator $[m^2]$;
- η_{STC}: Efficiency in STC conditions of the modules;
- P_N: Sum of the peaks powers of modules in STC condition $[W]$;
- h_{eq}: number of equivalent hour with 1000 kWh/m^2 irradiance [h];
- PR: Performance Ratio.

Another interpretation of the formula involves the concept of yield for estimating daily, monthly and annual yield :

$$E_{AC} = P_N \cdot Y_R \cdot PR = P_N \cdot Y_F \tag{20}$$

dove:

- Y_R:Reference yeld or peak solar hours (H_g/G_{STC} expressed in h/day, h/-month e h/year);
- Y_F: Final yeld (E_{AC}/P_N expressed in h/day, h/month e h/year);
- P_N: sum of nominal powers of the modules (in STC).

STC (Standard Test Condition): $G = 1000\,W/m^2$; $T_a = 25°C$; AM=1.5.
Various sources of losses (or rarely gains) are included in the PR, the main ones being:

1. Tolerance respect to STC datas and inherent mismatch of I-V characteristics of modules;
2. dirt and reflection of sunlight;
3. solar spectrum different from the reference spectrum (AM=1.5);
4. wiring, blocking diodes, fuses and switches;;

5. over/under temperature respect to $25°C$;
6. Non-uniform lighting on all modules (partial shading effect);
7. MPP tracker and DC/AC conversion of the inverter;
8. losses in the step-up transformer (if present).

$$PR = \eta_{mis} \cdot \eta_{d-r} \cdot \eta_{spec} \cdot \eta_{wir} \cdot \eta_{temp} \cdot \eta_{shad} \cdot \eta_{inv} \cdot \eta_{trans} \tag{21}$$

The parameters of the conventional yield formula are very hard to estimate, and this is a major flaw:

- PV module certification data are obtained from simulated light laboratory tests on a small sample of the population ($< 1\%$), flash reports are given without uncertainty by the manufacturer;
- the design value of the PR is 0.75, but the actual values lie in the range $0.55 \div 0.85$ depending on the quality of the hardware, software and particular environmental conditions in which the plant is installed;
- h_{eq} Is calculated using the 1994 UNI 10349 standard.

Eq.(20) will be used to calculate some range of yeld of the plant.

Two different scenario will be presented using as P_N values the actual value of peak power installed (12.251 kWp) and the maximum DC power in input to the inverter (10.061 kWp).

$$Y_R = \frac{H_g}{G_{STC}} = \frac{1844.1 \ \cdot \ 10^3}{1000} = 1874.6h \tag{22}$$

As can be seen from the values founded the estimate of energy yield can change a lot considering different PR values. The estimation has been carried out for two different values of installed power because the method does not take into account the NPR. Considering all of that probably the real power produced by the plant will be between 16031.30 and 19521.18 MWh/year. Since the evaluation of the yield of the plant is crucial also an estimate with the software PVGIS and an hourly estimate made considering the environmental conditions are made to make a comparison.

After finding the Y_R we can estimate the yield of the PV plant:

PR values	**Energy Yield [MWh/year]**	**Energy Yield [MWh/yaer]**
0.85	19521.18	16031.30
0.75	17224.57	14145.26
0.55	12631.35	10373.19
P_N [MW]	**12.251**	**10.061**

2.4 PVGIS-Based Simulation

To double check the results obtained with the "Annual Energy Production Estimation", it has been decided to use the software PVGIS[10](Photovoltaic Geographical Information System[23]), developed by the research center of the Institute for the Environment and Sustainable Development of the European Commission; it is one of the best for the estimation of the production of a photovoltaic plant.

PVGIS features includes:

- precise weather data and GPS defined information to calculate photovoltaic production. This allows for much more precise estimates than estimates based on general approximations;
- allows users to provide detailed information about their installation, for example type of solar modules, installed power, azimuth and tilt angles, etc. These specific data make it possible to obtain a personalized estimate of production and of the LCOE;
- By providing information on the optimal tilt and azimuth, PVGIS can help to improve the yield optimizing the design of your solar installation for maximum production;
- Once your solar installation is operational, you can compare actual results with the estimates provided by PVGIS to evaluate the performance of your system and identify potential deviations.

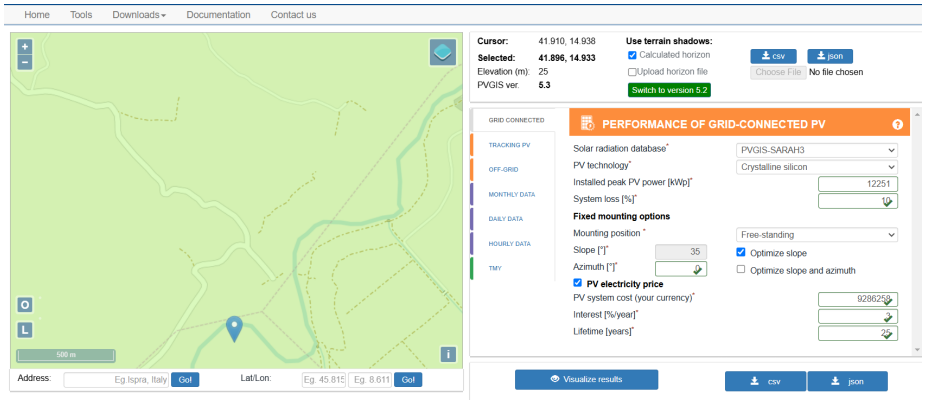

Figure 23: PVGIS graphical interface.

PVGIS requires some information in input in order to proceed in its estimation:

[10]PVGIS website

- Solar radiation database: PVGIS-SARAH3 uses the images of the two METEOSAT geostationary satellites giving information about European, Asian and African continents the hourly values are calculated from a satellite image;
- PV technology: Crystalline silicon;
- Installed peak PV power [kWp]: also in this case both values of peak power will be considered 12251,2 kWp and 10061 kWp; only for the first value the PVGIS interface will be showed but at the end of the section will be a table with all the values calculated;
- System loss [%]: estimated roughly at 10% (2.3% cable and connection losses, 2.2% inverter losses,2% mismatch between modules, 1.75% dirt losses, 1.75% front glass reflection);
- Mounting position: free-standing, meaning that the modules are mounted on a rack with air flowing freely behind the modules.

In Fig.24 there are the final results provided by the software:

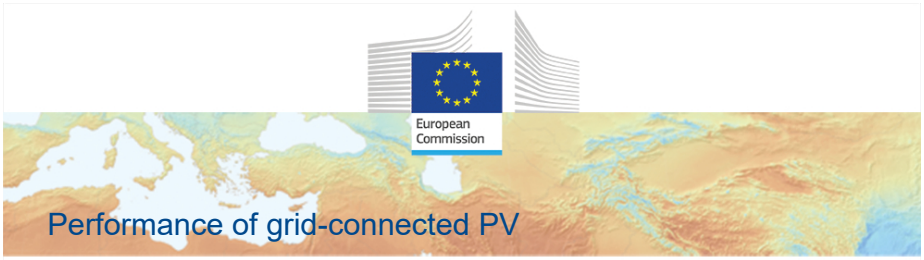

PVGIS-5 estimates of solar electricity generation:

Provided inputs:

Latitude/Longitude:	41.896,14.933
Horizon:	Calculated
Database used:	PVGIS-SARAH3
PV technology:	Crystalline silicon
PV installed:	12251 kWp
System loss:	10 %

Simulation outputs

Slope angle:	36 (opt) °
Azimuth angle:	-3 (opt) °
Yearly PV energy production:	18731769.39 kWh
Yearly in-plane irradiation:	1874.6 kWh/m²
Year-to-year variability:	607416.52 kWh
Changes in output due to:	
Angle of incidence:	-2.68 %
Spectral effects:	0.97 %
Temperature and low irradiance:	-7.77 %
Total loss:	-18.44 %
PV electricity cost [per kWh]:	0.030 per kWh

Outline of horizon at chosen location:

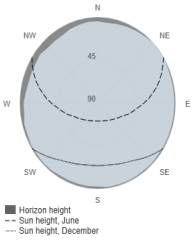

Monthly energy output from fix-angle PV system:

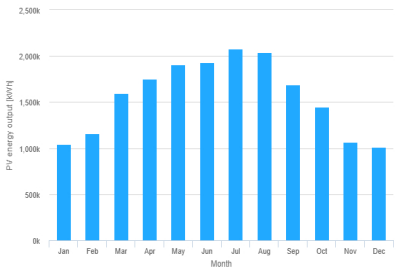

Monthly in-plane irradiation for fixed-angle:

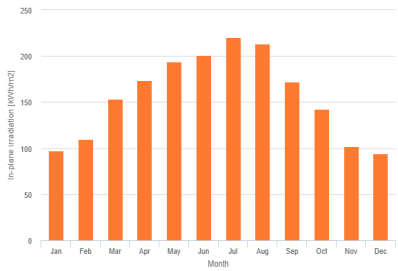

Monthly PV energy and solar irradiation

Month	E_m	H(i)_m	SD_m
January	1044896	97.5	232996.4
February	1162358	109.6	197462.3
March	1593276	148.8	189084.9
April	1750177	164.0	156992.8
May	1908353	179.7	166071.4
June	1933047	181.2	84177.3
July	2082772	190.2	90226.9
August	2037729	203.6	120847.7
September	1689113	171.9	121188.7
October	1451845	142.7	204496.0
November	1069216	102.3	160025.0
December	1008981	94.3	147315.9

E_m: Average monthly electricity production from the defined system [kWh].

H(i)_m: Average monthly sum of global irradiation per square meter received by the modules of the given system [kWh/m²].

SD_m: Standard deviation of the monthly electricity production due to year-to-year variation [kWh].

Report generated on 2025/02/26

Figure 24: PVGIS simulation results.

Impact of Solar Incidence Angles on Yield

The software is capable of finding the optimal Slope angle and Azimuth angle to maximize the yearly energy production combining weather data, irradiation data, and geographical data of the location selected. Slope angle is the angle of the PV modules from the horizontal plane, for a fixed (non-tracking) mounting. The azimuth angle, or orientation, defines the direction in which the PV modules face relative to true South. An azimuth of 0° means the modules are facing directly South, while -90° corresponds to East, and 90° to West.
The results for the case under study are shown in Tab.13:

Slope angle	36°
Azimuth angle	-3°

Table 13: Slope and Azimuth angles.

Energy Output Simulation

In Fig.25 there is a detail of the monthly energy production of the plant:

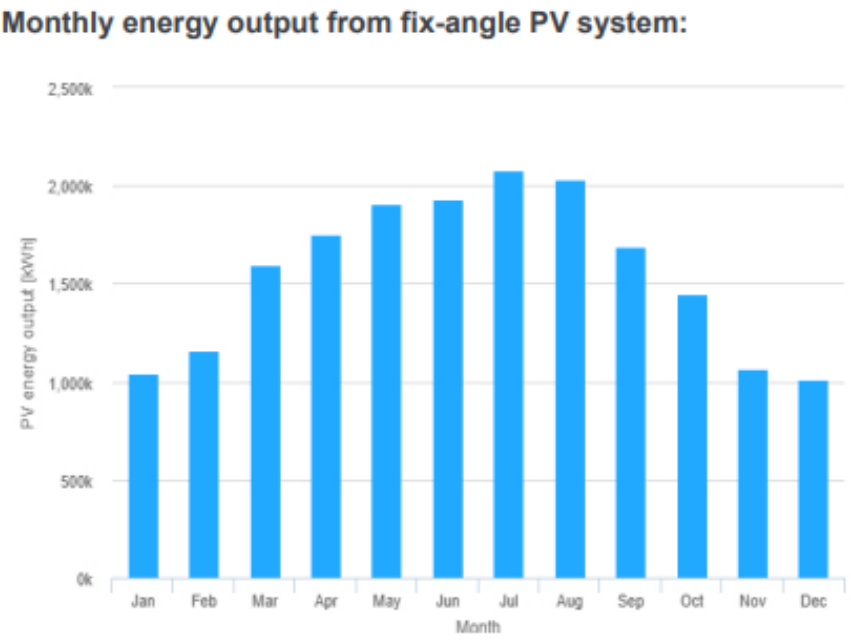

Figure 25: Average monthly energy output.

In Fig.26 there is a detail of the monthly irradiation on the site:

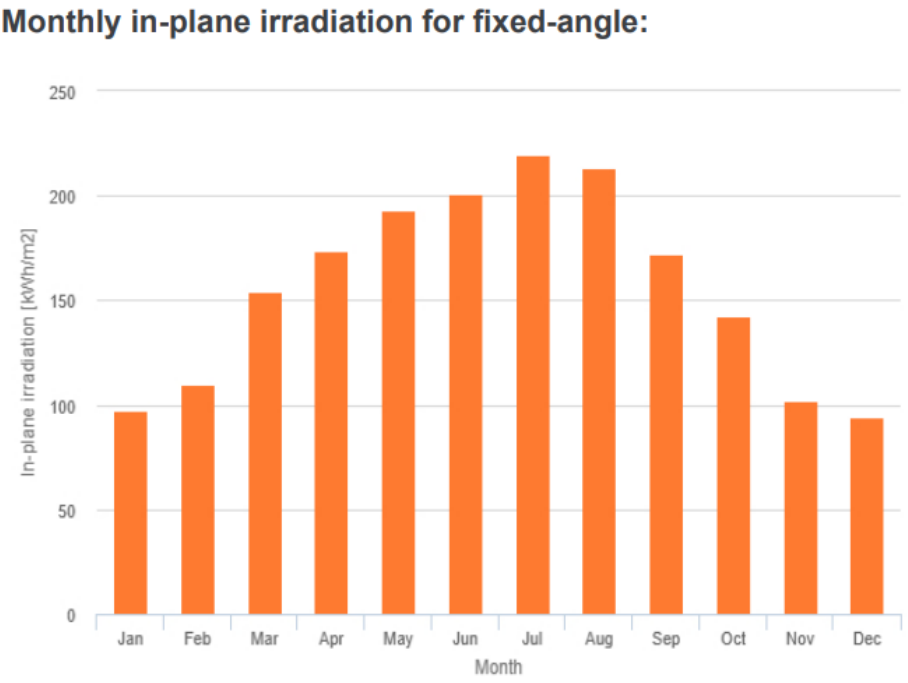

Figure 26: Average monthly irradiation.

The energy production goes from a minimum of 1009.21 MWh in December to a maximum of 2077.6 MWh in July. The annual estimated energy production is 18723 MWh with an year-to-year variability of 603 MWh: if this estimation is correct the annual production of the plant should stay below 4% of variation, and this relatively small variation will allow to stipulate bilateral contract to sell energy with a low risk of under-producing the latter. In Tab.14 the results of PVGIS monthly energy production and irradiance are summed up:

Month	**Production** E_m **[MWh]**	**Irradiance** $H(i)_m$ **[kWh/m²]**	**Standard deviation** SD_m **[MWh]**
January	1045	97.5	233
February	1163	109.7	197
March	1594	153.9	189
April	1750	173.9	157
May	1907	193.5	166
June	1928	200.8	84
July	2077	219.7	90
August	2035	213.3	120
September	1689	172.0	121
October	1452	142.8	204
November	1070	102.4	160
December	1009	94.3	147
Totale	**18731**	**1874.6**	-

Table 14: PVGIS results.

The energy production takes into account 18.44% of losses, and apart from the efficiency discussed before are included:

- 2.68% losses due to Angle of incidence;
- 7.77% losses due to temperature and low irradiance;
- 0.97% efficiency gain due to spectral effects.

In Tab.15 there are all the results obtained from the simulation:

Provided inputs:	
Location [Lat/Lon]:	41.896,14.933
Horizon:	Calculated
Database used:	PVGIS-SARAH3
PV technology:	Crystalline silicon
PV installed [kWp]:	12251
System loss [%]:	10
Simulation outputs:	
Slope angle [°]:	36 (opt)
Azimuth angle [°]:	-3 (opt)
Yearly PV energy production [kWh]:	18731769.39
Yearly in-plane irradiation [kWh/m2]:	1874.6
Year-to-year variability [kWh]:	607416.52
Changes in output due to:	
Angle of incidence [%]:	-2.68
Spectral effects [%]:	0.97
Temperature and low irradiance [%]:	-7.77
Total loss [%]:	-18.44
PV electricity cost [per kWh]:	0.030

Table 15: 12.25 MWp simulation.

In Tab.16 there are all the results obtained from the simulation considering as installed peak power 10.06 MW:

Provided inputs:	
Location [Lat/Lon]:	41.896,14.933
Horizon:	Calculated
Database used:	PVGIS-SARAH3
PV technology:	Crystalline silicon
PV installed [kWp]:	10060
System loss [%]:	10
Simulation outputs:	
Slope angle [°]:	36 (opt)
Azimuth angle [°]:	-3 (opt)
Yearly PV energy production [kWh]:	15381732.11
Yearly in-plane irradiation [kWh/m2]:	1874.6
Year-to-year variability [kWh]:	498784.61
Changes in output due to:	
Angle of incidence [%]:	-2.68
Spectral effects [%]:	0.97
Temperature and low irradiance [%]:	-7.77
Total loss [%]:	-18.44
PV electricity cost [per kWh]:	0.036

Table 16: 10 MWp simulation.

From this second analysis the yield estimate are between 18732 MW/year considering a peak power installed of about 12.25 MW and 15382 MW/ year considering a peak power installed of about 10.06 MW.

Price for electricity

The estimated cost for electricity is 0.03 €/kWh or 30 €/MWh in the first scenario and 0.038 €/kWh or 38 €/MWh in the second scenario. This difference derives from the fact that the overall cost is the same in the simulations while the energy production is higher in the first scenario. These prices is a LCOE that take into account:

- Total Installation Cost: that includes hardware costs (modules, inverters, racking and mounting, grid connection, cabling/wiring, safety and security, monitoring and control), installation costs (such as mechanical installation, electrical installation inspection) and soft costs (profit margin,financing costs, system design, permitting, incentive application, customer acquisition);

- Interest rate on financing: If a loan is required to finance the PV system, the interest rate applied plays a crucial role.

  The calculation assumes a fixed interest rate, with the loan being repaid through annual installments over the system's lifetime (25 years).

In case the plant does not request financing this share of the LCOE could be intended like opportunity cost of the investment; anyway the economical considerations will be deepened in Sec.4.1;

- System lifetime: the expected operational lifetime of the PV system heavily affects the final electricity cost. A longer system lifespan leads to a lower electricity cost per kWh, as the initial investment is spread over a greater number of years.

2.5 Proposed Estimation of the Yield

With the design choice made in Sec.2.2 the total kW_p installed is given by:

$$P_{DC,array} = n_{STR} \cdot n_{MODSTR} \cdot P_{max,STC} = \frac{260 \cdot 19 \cdot 620}{1000} = 3061 \ kW \quad (23)$$

So the real NPR of the plant will be:

$$NPR = \frac{P_{DC}}{P_{DC,array}} = \frac{2510.14}{3061} = 0.82 \quad (24)$$

As illustrated in Sec.2 there are a lot of advantages in increasing the number the DC power of modules compared to the maximum DC input power of the inverter, on the other hand, during a certain window of time, there will be a curtailment of the exceeding energy because everything is working at maximum power, the irradiance is higher than 1000 W/m^2 and the temperature is lower or equal to 25°C of STC; this situation is more likely to happen in spring or autumn, since in winter irradiance is considerably lower and in summer, when irradiance is higher than STC, the temperature (on the module) is likely to be higer than STC, with a consequent power output derating of -0.280 %/°C. Lets describe how energy curtailment is realized: since the inverter has a fixed maximum power rating, it cannot convert and inject more power into the grid beyond that limit.

To avoid overloading, the inverter actively limits the power it draws from the PV array by adjusting its Maximum Power Point Tracking (MPPT) algorithm. What happens in practice is that the inverter shifts the operating point of the PV system in a way that reduces the current it extracts from the modules, effectively keeping the input power within its design limits. This means that even though the solar modules could generate more energy, the inverter ensures that it only processes up to its rated capacity. As a result, there is no increase in power output beyond the inverter's nominal rating.

The excess energy that could have been extracted is simply not utilized, leading to a reduction in the overall efficiency of the photovoltaic system. However, this process does not cause any damage to the inverter or the solar modules, as the power regulation is handled automatically by the inverter's control system. Since PVGIS gives the possibility to have data about irradiation (G(i)), air

temperature (T2m) and wind at 10 meters above the ground (WS10m) starting from 1st january 2005 to 31st december 2023, to have an idea of the NPR impact on the energy production lets suppose that for the next 19 years we can expect the same wheatear behavior. The idea is to use hourly data from PVGIS and combining some simplified equations Using an excel spreadsheet to make an estimation that will take into account as many variables as possible. The equation that will be used are: Eq.(25) proposed by Skoplaki et al.[24] and Eq.(26):

$$T_{cell} = T_a + \frac{G}{G_{NOCT}} \cdot (T_{NOCT} - T_{a,NOCT}) \cdot \frac{h_{w,NOCT}}{h_w(v)} \cdot \left[1 - \frac{\eta_{STC}}{\tau a} \left(1 - \gamma_{\mathrm{Pm}} T_{STC}\right)\right] \tag{25}$$

$$P_{DC}(G, Tc) = P_{DC,array} \cdot \frac{G(i)}{1000} \cdot [1 + \gamma_{\mathrm{Pm}} \cdot (T_{cell} - 25)] \tag{26}$$

The standard approach to find the cell temperature uses Eq.27:

$$T_{cell} = T_{air} + (T_{NOCT} - 20) \cdot \frac{G(i)}{800\ W/m^2} \tag{27}$$

Instead the equation proposed by Skoplaki et al. considers also: the efficiency η_{STC} of the module, the temperature coefficients of $\mathrm{P}_{max})\gamma_{\mathrm{Pm}}$ (that in the original paper is called β_{STC}), the absorption coefficient of the cells α and the transmittance of the cover system τ (represents the fraction of incident light that passes through the cover system). The value of $\tau \cdot \alpha$ can be assumed as 0.9. η_{STC} and γ_{Pm} are the values reported in Tab.10 and are given in STC conditions, the last parameter h_w is the wind convection coefficient (h_{wNOCT} wind convection coefficient in NOCT conditions), for this coefficient Sklopaki et.[24] proposed two different equations:

$$h_w = 8.91 + 2.00 \cdot v_f \tag{28}$$

$$h_w = 5.7 + 2.8 \cdot v_w \tag{29}$$

the difference between (28) and (29) is that the first one use v_f the wind speed measured at 10 m above ground level, while the first one use v_w the wind speed measured at 2 meters above ground level, so near the modules.

The approach proposed by Skoplaki et al. is not the only one possible, there are different semi-empirical formulas to estimate cell temperature. This approach has been chosen after studying another paper written by Schwingshackl et al.[11] in which the authors use different equations proposed by different studies to estimate the temperature of the PV cells. The case under study in the paper written by Schwingshackl et al.[11] is a multi-tecnology generation plant located at Bolzano, Italy (46°27'28" N, 11° 19'43"E, 247 meters above sea level) equipped with anemometers to measure wind speed, solarimeter to measure solar irradiance and thermometers to measure the air temperature. They

compared the result obtained using Sklopaki equation with the in-situ datas and with data from ECMWF (European Centre for Medium-Range Weather Forecasts). From the analysis emerged that using (25) and (28) together to:

$$v_w = 0.68 \cdot v_f - 0.5 \tag{30}$$

used for transforming from the wind speed at 10 m to the wind speed at 2 meters,the wind speed is saturated to zero if it is negative from Eq.30. The final result of the study are expressed with two different statistical metrics: R^2 (coefficient of determination) and **RMSE** (Root Mean Squared Error) that are used to evaluate the performance of photovoltaic cell temperature prediction models. Their formal definitions and interpretations:

$\mathbf{R^2}$: Coefficient of Determination

The coefficient of determination quantifies the proportion of variability in the observed data explained by the model. It is defined as:

$$R^2 = 1 - \frac{SS_{\text{res}}}{SS_{\text{tot}}} \tag{31}$$

where:

- $SS_{\text{res}} = \sum_{i=1}^{n}(y_i - \hat{y}_i)^2$ is the residual sum of squares (squared differences between measured values y_i and predicted values $\hat{y}_i$),
- $SS_{\text{tot}} = \sum_{i=1}^{n}(y_i - \bar{y})^2$ is the total sum of squares, with $\bar{y}$ as the mean of measured values.

RMSE: Root Mean Squared Error

RMSE measures the average magnitude of prediction errors, penalizing larger errors more heavily. Its equation is:

$$RMSE = \sqrt{\frac{1}{n}\sum_{i=1}^{n}(y_i - \hat{y}_i)^2} \tag{32}$$

where n is the number of observations.

Interpretation of Results

- **High R^2 + Low RMSE**: Indicates an accurate model.
- **Low R^2 + High RMSE**: Suggests a less reliable model.

in-situ wind data				**ECMWF wind data**	
		hourly mean		hourly mean	
Model	Technology	R^2	RMSE (K)	R^2	RMSE (K)
Standard	m-Si	0.77	7.8	0.77	7.8
Skoplaki 2	m-Si	0.97	2.3	0.92	3.9

Table 17: Results of the Schwingshackl et al.[11] paper.

The final conclusion of the paper are:

1. The Sklopaski 2 model seems to be the best for estimating cell temperature of m-Si in the case under study;
2. as shown from the values of R^2 and RMSE the wind has a strong impact on the estimation of the temperature of the cell;
3. it is not possible to find a general formula to estimate module temperature since the performance of different models varies between different modules technologies;
4. data from ECMWF are a good approximation when in-situ data are not available, the result obtained are less accurate but they are still a lot better than the one obtained with standard model.

The authors of the study also specify that their model is not general and further experiments are needed to extend this results in different conditions. Even if the method is not general since this model is used in the thesis to improve the accuracy of the cell temperature estimation.

The parameter utilized in Eq.(25) and Eq.(26) are:

- T_c = cell temperature (estimated with Skoplaki);
- T_a = air temperature (from PVGIS dataset);
- G(i) = hourly average irradiance (from PVGIS dataset);
- G_{NOCT} = hourly average irradiance (from PVGIS dataset);
- T_{STC} = 25°C temperature in standard conditions;
- T_{NOCT} = 45°C nominal operating cell temperature;
- $T_{a,NOCT}$ = 20°C nominal operating cell temperature;
- η_{STC} = 23% efficiency in STC of the module (from module datasheet);
- γ_{Pm} = -0.28 %/°C the temperature coefficients of P_{max} (from module datasheet);
- α the absorption coefficient of the cells;

- τ transmittance of the cover system ;
- $P_{DC,array} = 3061$ kW is the DC peak power of the photovoltaic array.

In Tab.18 are presented the total of hours, days and years[11] analyzed, as said before the period of the analysis goes from 1st January 2005 to 31 December 2023; for the final 6 years of life of the implant the data are estimated through linear interpolations of previous data and through more qualitative considerations.

Total hours analyzed	**Days Analyzed**	**Years analyzed**	**Productive hours**	**Hours in which irradiance is greater than zero (G>0)**
166536	6939	19,011	79869	81692

Table 18: Total of hours analyzed starting from 1st January 2005 until 31st December 2023.

Tab.19 provides a comprehensive overview of the yield and performance data of the photovoltaic plant over a period of 19 years, with some projections extending to 25 years, the total productive hours of the plant are only the hours when the PV array (considering losses) produce at least the threshold power of the inverter equal to 25 kW, below this value the inverter stays disconnected from the grid.

Data about yield of the plant		
Parameter	**Value**	**Percentage value respect total**
$P_{DCmax,inv}$ [kW]	2510	
NPR (Nominal Power Ratio)	0.82	
P_DC,array [kW]	3061	
Hours in which $P_{DC,input,inv} \geq 2510$ kW (in 19 years)	2756	3.45 %
Energy over-production (in 19 years) [MWh]	272	0.242 %
Total energy produced by one array (in 19 years subtracting over-production)[MWh]	90820	
Total energy produced by 1 inverter (in 19 years) [MWh]	87063	
Total energy injected into the grid (in 19 years) [MWh]	86193	
Energy injected into the grid by one production unit (averaged on 19 years) [MWh]	4536.5	
Energy injected into the grid from 4 production units (25 years) [GWh]	448.968	

Table 19: Data about yield of the plant.

[11] the unusual 19.011 years is caused by leap years

- Maximum DC Power of the Inverter ($P_{DCmax,inv}$):
  - The inverter has a maximum DC power capacity of **2510 kW**, which represents the upper limit of power it can handle in input.
- **DC Power of the Array ($P_{DC,array}$)**:
  - The Photovoltaic array, that feeds one inverter, has a total DC power output of **3061 kW**, which is higher than the inverter's maximum capacity. This implies that the MPPT of the inverter will limit its input power when necessary.
- **Hours of Inverter Saturation**:
  - The inverter operates at or above its maximum capacity for **3344 hours** over 19 years, representing **3.45%** of the total operational time. Such instances are relatively rare and if we consider the last six years of operation projection the 3.45% figure is likely to decline.
- **Energy Over-Production**:
  - Over 19 years, the system experiences **272 MWh** of energy over-production, which accounts for **0.242%** of the total energy produced. This over-production occurs when the PV array generates more power than the inverter can handle.
- **Total Energy Produced by One Array**:
  - Excluding over-production, a single array produces **90820 MWh** over 19 years.
- **Total Energy Produced by One Inverter**:
  - A single inverter generates **87063 MWh** over the same period. The difference between the array and inverter outputs is due to the loss coefficients given in the Tab.20.
- **Total Energy Injected into the Grid**:
  - The total energy injected into the grid over 19 years is **86193 MWh**, slightly lower than the total energy produced by the inverter. This difference is due to transformer efficiency.
- **Annual Energy Production (Averaged over 19 Years)**:
  - On average, one inverter produces **4582 MWh** per year, while the energy injected into the grid averages **4536.5 MWh** annually.
- **Energy Injected into the Grid from 4 Production Units (25 Years)**:

– Over a 25-year period, the four production units collectively inject **448.968 GWh** into the grid.

In Tab.20 all the possible source of losses are presented with their calculated or estimated value:

Possible Sources of Loss		
Coefficient	**Description**	**Value (η)**
η_{mis}	Mismatch and module tolerances	0.970
η_d	Dirt on the front glass	0.976
η_r	Reflection of the front glass	0.971
η_{wir}	Losses in cables, diodes, fuses, and switches	0.9768
η_{temp}	Losses due to temperature	0.9375
η_{spec}	Solar spectrum different from AM=1.5	1
η_{shad}	Losses due to shading	0.98
η_{inv}	Losses in the inverter and MPP tracker	0.978
η_{trasfo}	Transformer efficiency	0.990
PR	**Performance Ratio**	**0.807**

Table 20: Possible Sources of Loss and Performance Ratio.

Since the results presented in Tab.19 are strongly conditioned by the coefficients presented above, is important to describe them and to say where and when they were used in the calculations[12]:

- **Mismatch and Module Tolerances (η_{mis})**:
  - This coefficient accounts for losses due to mismatches between PV modules and manufacturing tolerances. The power output tolerance given from the producer is from 0 to 3%, for this parameter we assume the worst case scenario so η_{mis} **is assumed 0.97**. Since the mismatch effect is always present the loss of efficiency is directly applied to P_DC,array [kW].
- **Dirt on the Front Glass (η_d)**:
  - Dirt dust and sand accumulation on the surface of PV modules reduces their ability to efficiently convert sunlight into energy. The coefficient of **0.976** taken from the scientific literature and is directly applied to P_DC,array [kW].
- **Reflection of the Front Glass (η_r)**:
  - Although the module surface is coated with anti-reflective materials a considerable portion of sunlight is still reflected leading to a loss of efficiency. The coefficient of **0.971** taken from the scientific literature and is directly applied to P_DC,array [kW].

[12]The excel spreadsheet attached to the thesis contains all the detailed mathematical passages.

- **Losses in Cables, Diodes, Fuses, and Switches (η_{wir})**:
  - Electrical losses in the wiring and other components of the PV system are represented by this coefficient. The value of **0.9768** is calculated in the thesis and is directly applied to P_DC,array [kW].
- **Losses Due to Temperature (η_{temp})**:
  - Temperature-related losses usually are one of the most important inefficiency cause, in this case (η_{temp}) is about **0.9375**. The losses due to temperature are taken into account directly in Eq.(26).
- **Solar Spectrum Different from AM=1.5 (η_{spec})**:
  - The PV modules are designed for a standard solar spectrum (AM=1.5). This coefficient is supposed one because the irradiance data of PVGIS should already consider its effect.
- **Losses Due to Shading (η_{shad})**:
  - Shading from: nearby objects, other modules rows (at morning and sunset), small clouds passages and vegetation reduces the energy output of the Photovoltaic system. The coefficient (η_{shad}) is one of the most difficult, PVGIS in its irradiance data already considers the shadows created by very large clouds or mountains, but does not consider the small clouds and the partial shading caused by the rows of modules in the morining and at sunset. The value of **0.98** is chosen from the scientific literature.
    To not underestimate the over-production this coefficient and the one that will follow are applied directly to the "Total energy produced by one array (in 19 years subtracting over-production)" to obtain the "Total energy produced by 1 inverter (in 19 years)".
- **Losses in the Inverter and MPP Tracker (η_{inv})**:
  - The inverter to perform the DC/AC conversion introduce conductive and switching losses. Furthermore the MPP tracker algorithm introduce additional losses. A coefficient of **0.978** is chosen and is applied as explained in the "Losses Due to Shading" point.
- **Transformer Efficiency (η_{trasfo})**:
  - The transformer used in the system has an estimated efficiency of **0.99**, this efficiency is taken into account to calculate the effective power injected into the grid.
- **Performance Ratio (PR)**:
  - The overall performance ratio of the system is **0.806**, which means the system operates at **80.6%** of its theoretical maximum efficiency. This value is the product of all individual coefficients[13] and reflects

[13] Excluding the efficiency of the transformer as indicated in IEC 61724 standard

the cumulative impact of all losses.

Inverter Performance

To get graphical feedback about the inverter performance in the following figures are presented some trends concerning the inverter load and the tend of over-production hours during the years:

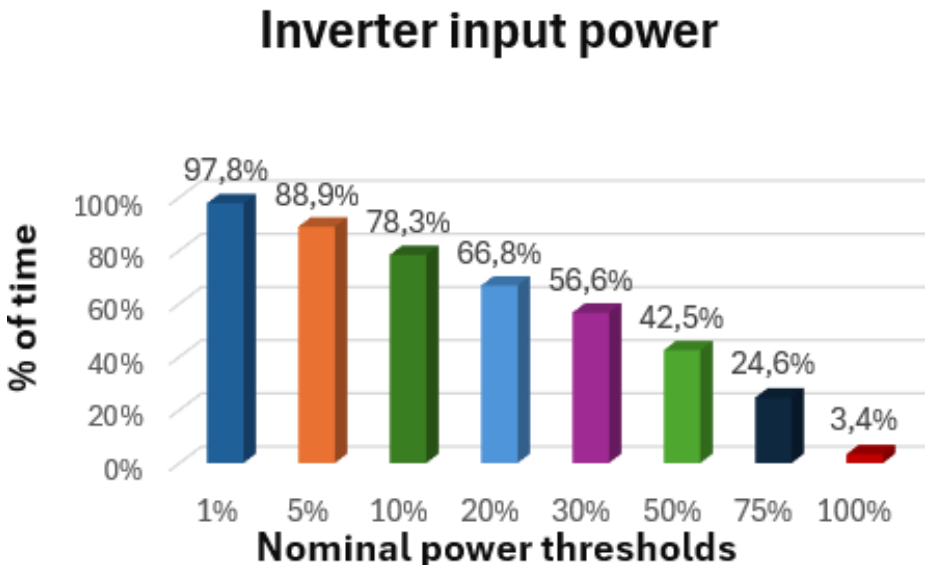

Figure 27: Inverter minimum loads.

In Fig27 y-axis shows the percentage of time in which a minimum load is achieved while the x-axis shows the minimum percentage of nominal power in input to the inverter (e.g. 5% rated power 10% rated power etc.). In the 19 years analyzed the inverter minimum load operate over 75% or more of its nominal power only for the 24.6% of the time[14].

[14]The total time considered is only are only the hours of the day in which the array power is higher than 25 kW.

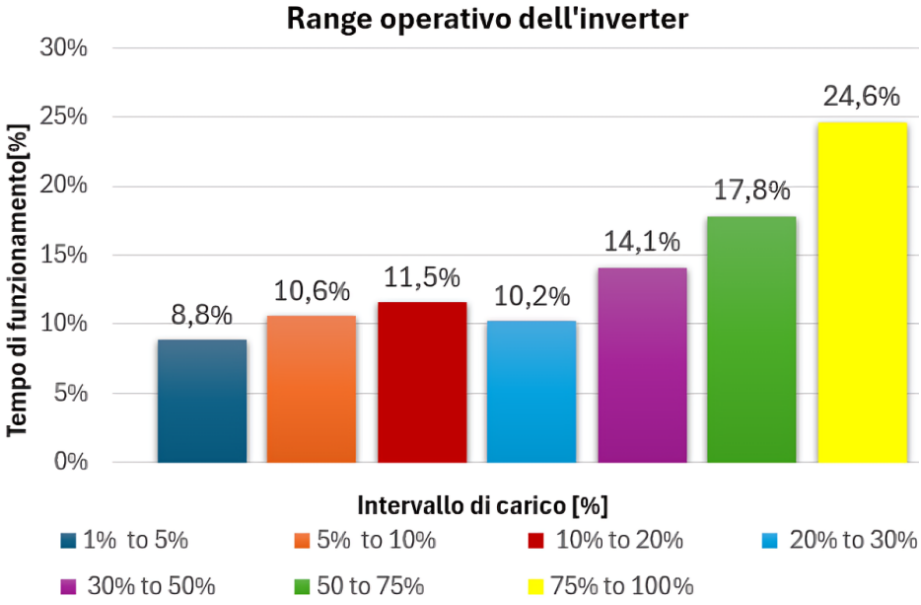

Figure 28: Inverter 3061 kWp load range.

In Fig.28 are presented the the periods of time in which the inverter operate in a certain load range (e.g. from 50% to 75% of nominal power). This information is very useful for the analysis because give an idea of the real load range that the inverter will experience during the first 19 years of operation. This values (together to the MPPT system) are the reason for which the efficiency estimated for the inverter is only 97.8% and not the European Efficiency of 98.4% given from the producer, actually European efficiency is calculate with a weighted average Eq.(33):

$$\eta_{EU} = 0.03 \cdot \eta_{5\%} + 0.06 \cdot \eta_{10\%} + 0.13 \cdot \eta_{20\%} + 0.10 \cdot \eta_{30\%} + 0.48 \cdot \eta_{50\%} + 0.20 \cdot \eta_{100\%} \quad (33)$$

but using the data from the simulation the weights of the 5% and 10% are under-estimated while the one of the 100% is over-estimated.

Unfortunately the producer does not give the efficiency curve of the inverter in function of its load, but considering that the typical efficiency profile of an inverter is the one showed in Fig.29 and the efficiency decrease strongly for loads below 20% a precautionary extra-loss of efficiency of 0.4% is applied to η_{EU} given from the producer[15].

[15] Usually the inverter does not start to produce energy

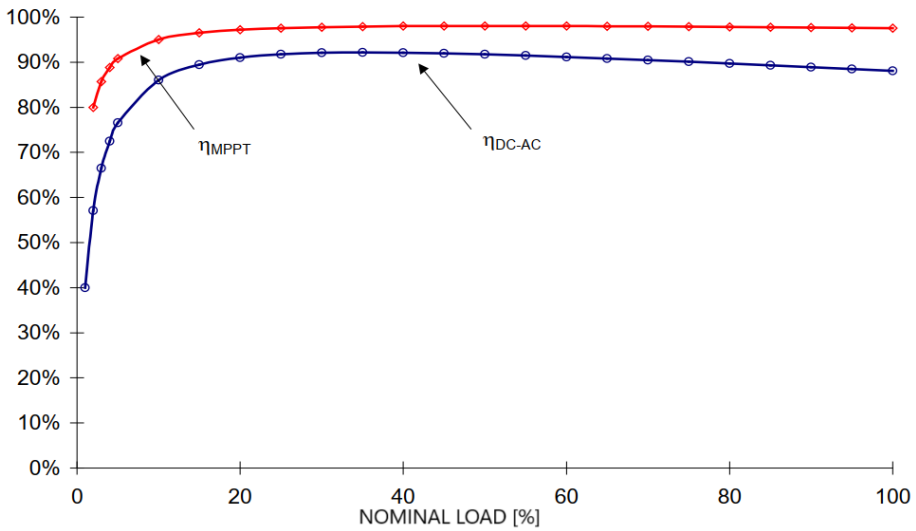

Figure 29: Typical Inverter efficiency profile.

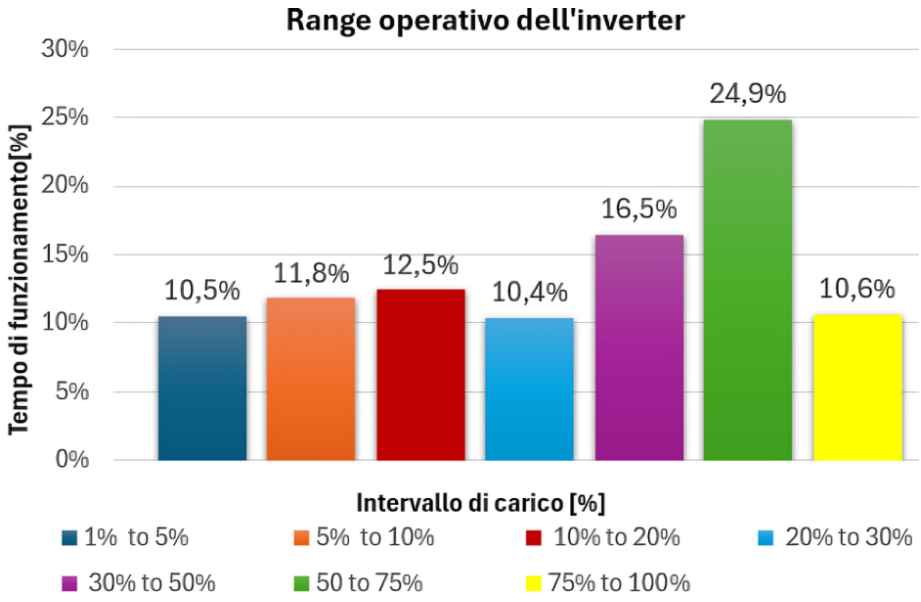

Figure 30: Inverter 2510 kWp load range

In Fig.30 in possible to see that with a power installed of 2510 kWp in STC, the operating hours at power levels below 20%, where the inverter efficiency drops significantly, decrease by 3.9%, while the operating hours at power levels above 75% increase by 14%.

3 Design and Optimization of Grid-Connected Photovoltaic Plants

3.1 Land Use Evaluation

In this section, the space that the plant would need is analyzed. Obviously, the goal is to use the lowest land use possible, still granting an optimal solar irradiation to all the modules. A "rule of thumb" utilized for small plant is to space the string of modules (or rows of modules) of 3 times the length of the single module, but this approach could lead to land use higher than the one actually needed. On the other end under estimating the space needed could be very counter productive in the case under study since it can cause the partial shading of the modules due to the shadow cast by other modules, and the centralized inverter that has to manage a lot of modules could lower its efficiency in a considerable way. The procedure adopted to rationalize the choice of the distance of rows will make use of sun path charts[25][16]. A Sun Path Chart is used for:

- Determining the Sun's trajectory The chart shows the altitude (angular height above the horizon) and azimuth (direction relative to north) of the Sun at different hours of the day and for various dates throughout the year. This helps to understand how sunlight varies over time;
- optimizing the orientation and tilt of photovoltaic modules;
- the sun Path chart allows us to identify the Sun's height on critical days (solstices and equinoxes). With this information, we can determine the minimum spacing between PV rows to avoid self-shading during peak production hours;
- Analyzing shading caused by nearby obstacles.

[16] Source: Sun Earthtools.com

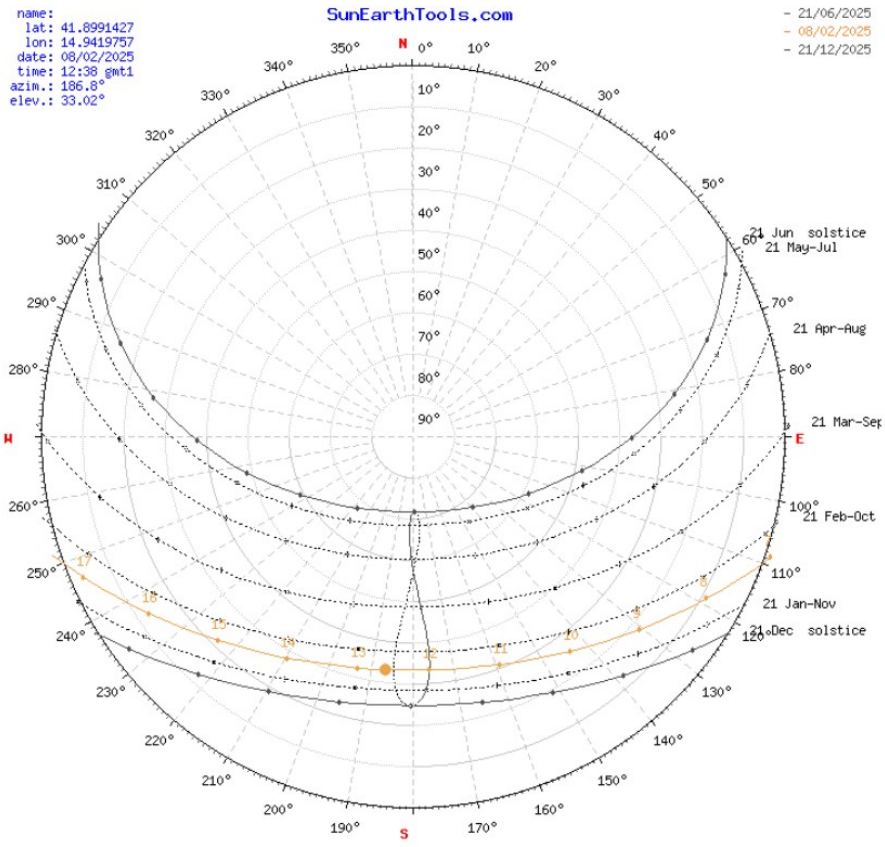

Figure 31: Compass sun path.

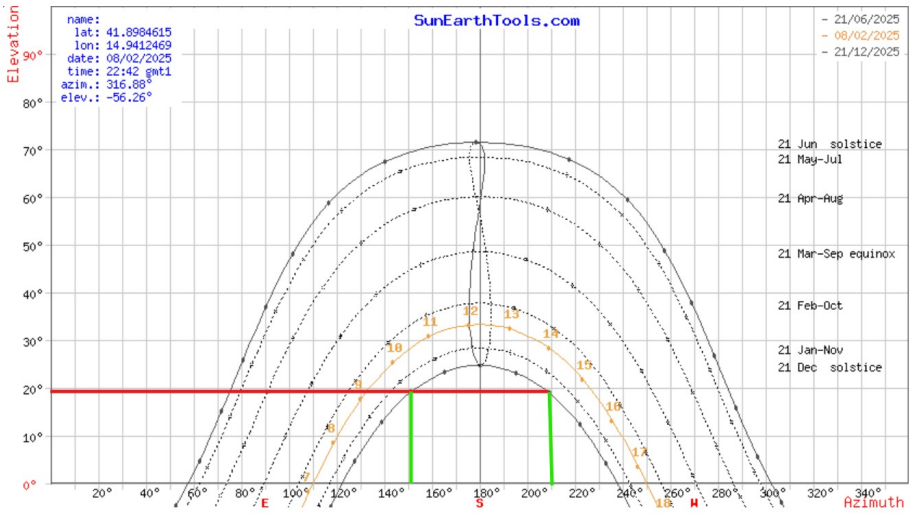

Figure 32: Sun path map.

To interpret the chart in Fig.32 the following considerations are made:

- The curves represent the sun's trajectory during different months (solstices and equinoxes are highlighted with their correspondent day of the year):
- The vertical axis shows the solar altitude (from 0° at the horizon to 90° at the zenith);
- The horizontal axis represents the azimuth (direction of sunlight relative to cardinal points);
- The hour lines indicate the Sun's position at different times of the day.

For the calculation we assume as a reference the lowest curve on the graph that correspond to 21 December (winter solstice), this is the day of the year in which in the northern hemisphere the sun has its lowest path on the horizon. In Fig.33 there is a side view of two rows of modules, that will be used as graphical reference for calculations.

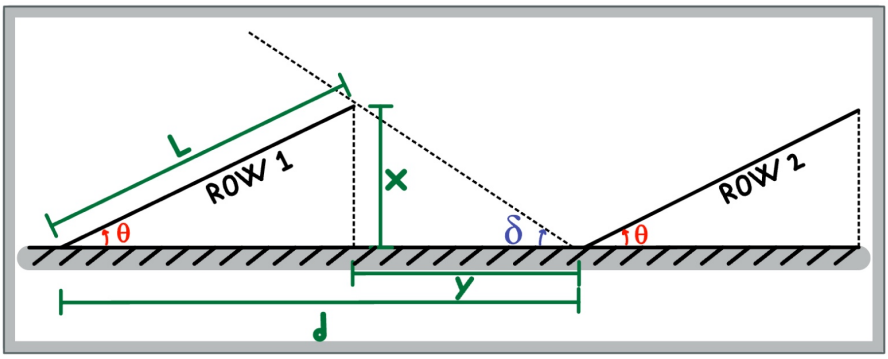

Figure 33: Trigonometry of row spacing.

Let's start introducing the parameters of the problem:

- L=2382 mm, is the length of the module taken from datasheet in Sec.15;
- X is the hight of the module from the ground (or better from the mounting platform);
- θ=36° is the optimal tilt angle obtained from PVGIS;
- $\delta \approx 19°$ is the angle of incidence of sun rays.
- d = distance between the beginning of row 1 and the beginning of raw 2

From Fig.32 we obtain three angles $\delta \approx 19°$ (obtained from the intersection of 10 AM point on 21 December curve and the elevation of the sun, Am=150 ° and As=180 ° that are the azimuth angles at 10 AM and at 12 AM. Now that the problem is defined with some trigonometric calculation we can find distance d:

$$d = L \cdot cos(\theta) + \frac{X}{tan(\delta)} = L \cdot cos(\theta) + \frac{L \cdot sin(\theta)}{tan(\delta)} \tag{34}$$

this formula would be correct if this was a bidimensional problem but since there is also the azimuth angle a correction factor must be added and Eq.(34) becomes [26]:

$$d = L \cdot [cos(\theta) + \frac{sin(\theta)}{tan(\delta)} \cdot cos(Am - As)] = 2.382 \cdot [cos(36°) + \frac{sin(36°)}{tan(19°)} \cdot cos(150° - 180°)] \approx 5.45\, m \tag{35}$$

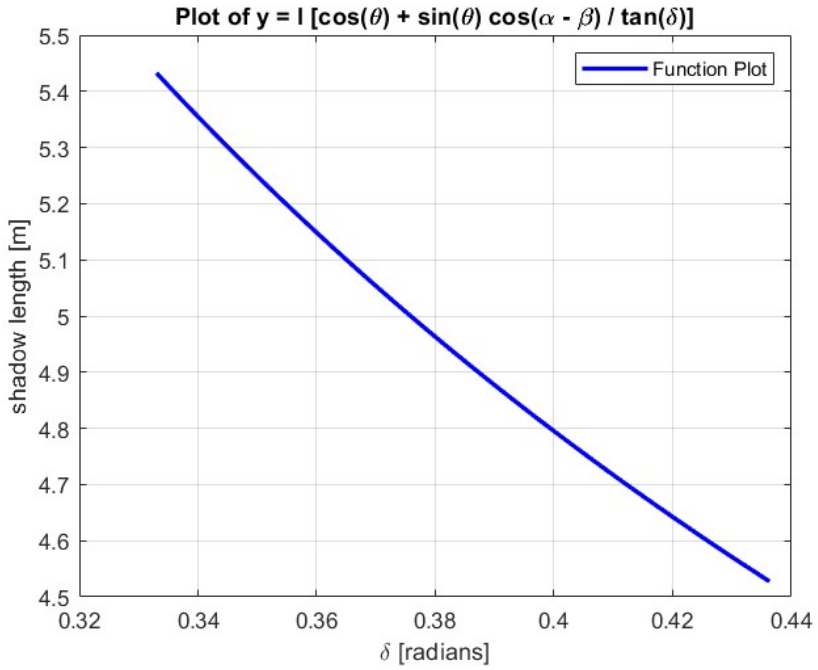

Figure 34: Shadow length during 21 December with
$19° \leq \delta \leq 25°$ (19° correspond to 10 AM 25° correspond to 12 AM).

In the previous Fig.34, the evolution of the shadow length projected by the modules is represented; this result guarantees that in the worst possible case, between 10 AM and 2 PM (hours of maximum electricity production), the array does not forecast shadows on itself.

Ground cover ratio

Considering the whole string, comprising 19 modules in series, the total length of the set is calculated with:

$$D = 18 \cdot d + L \cdot cos(\theta) = 18 \cdot 5.45 + 2.382 \approx 100.5 \ m \tag{36}$$

about 34 m. The total width of the set of module is calculated with:

$$W = (w + 0.05) \cdot 260 = (1.134 + 0.05) \cdot 260 \approx 308m \tag{37}$$

where:
w is the width of the single module and the extra 5 cm are space between each module needed to: facilitate the maintenance, improve the ventilation and to avoid failures due to thermal expansion.

In Tab.21, the dimensions of an array of strings (in the plant there are a total of 4 arrays(or sets, one for each inverter) are reported. This is the total measure

of the Photovoltaic array (only modules; transformer, inverter and DC combiner boxes are not included even because the area they occupy is negligible).

The ground cover ratio is calculated as:

$$GCR = \frac{area\ PV\ array}{area\ total\ ground} = \frac{19 \cdot 260 \cdot 2.382 \cos(36^\circ) \cdot 1.134}{100.5 \cdot 308} = 34.24\% \quad (38)$$

A high GCR means higher system cost (more land, longer cables, more joule losses, higher installation cost), while low GCR means lower system cost but larger shade that means less electricity produced.

The GCR obtained is a good compromise to balance both instances.

Length	100.5 m
Width	308 m

Table 21: Dimensions of the arrays.

3.2 Cable and Protection Sizing Criteria

DC Side Cabling and Voltage Drop Considerations

The cables in the photovoltaic plant must be able to withstand, for all the useful life of the plant (25 years), severe working conditions in terms of high temperature, atmospheric precipitation and ultraviolet radiation.

There are two kind of cables in the plant:

1. Solar cables (or string cables) that connect the modules to each other and the string to the combiner box: they are installed on the back of the modules themselves and must therefore withstand high temperatures (70-80°C) and resist ultraviolet radiation if installed in exposed locations.

2. Non-solar cables used downstream of the combiner box: they operate in ambient temperatures not exceeding 40°C, as they are located away from the modules. These cables lack UV resistance because are installed inside conduits to protect them.

The conduit on DC side of the plant must have double or reinforced insulation (class II); as for the cable installed downstream of the inverter the same consideration made for non solar DC cables can be made.

The operating current for a string in normal operating conditions is close to short circuit current, and it is assumed to be:

$$I_b = 1.25 \cdot I_{SC} = 1.25 \cdot 15.14 = 18.925\,A \quad (39)$$

where I_{SC} is the short-circuit current under standard test conditions. The 25% increase accounts for irradiance exceeding 1 kW/m^2

The cables connecting the DC combiner boxes to the inverter must carry an operating current:

$$I_{b,DCbox} = n \cdot 1.25 \cdot I_{SC} = 20 \cdot 1.25 \cdot 15.14 = 378.5\,A \tag{40}$$

where n is the number of strings in the DC combiner input.

DC Combiner Boxes

In ground-mounted solar power plants, inverters are installed at a central point, while DC combiners are spread out across the photovoltaic module field.

This results in short cable runs between the inverters and the transformer, meaning there is only minimal power loss on the AC side.

The DC combiner box chosen is from "Kaco new energy"[17] and has bipolar fuses on the input side and a switch disconnector on the output side other than embedded SPD (surge protection device class II).

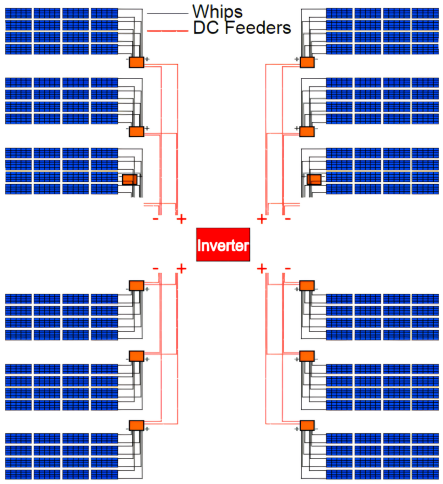

Figure 35: Combiner boxs and inverter layout.

In Fig.35 the layout of the plant is showed. This layout is compact and minimize the overall resistive losses in the cables.

[17] DC combiner box

Maximum no-load voltage	1,500 V
Maximum input current	20 A
Switch disconnector breaking & making capacity	400 A
Number of DC-string connections	20
String monitoring	
Measurement range - voltage	450 - 1500 V
Voltage measurement tolerance	0.5 %
Interfaces	RS485 (Modbus RTU), 4 x digital input
Control units	Status display and 4 buttons for local operation
Number of measuring channels	up to 20
Self-consumption	3 W
General data	
DC connection (input)	Direct connection
DC connection (output)	Max. Cable section 240 mm^2 (0.372 in^2) Cu or Al
Ambient temperature	-20 °C - + 40 °C
Humidity	0 - 95 %
Maximum installation elevation (above sea level)	2,000 m
Protection class	IP65
Protection fuses positve and negative	20 A
Dimensions (H x W x D)	835 x 1050 x 360 mm

Table 22: DC combiner box data.

Thermal Criteria

Cable lines are made of conducting material (copper or aluminum), insulated with insulating material (PVC, EPR, HEPR etc.).

The capacity of the cable is limited by the heat to be dissipated by the Joule effect, which can raise the temperature. The high temperature does not bring the conducting material of the cable under stress as much as the insulating material. The main limit is the temperature that the insulating material covering the conducting material of the cable itself can reach.

Before going into the details of cable sizing, some fundamentals quantities

are defined:

- I_z: maximum current that cable can transmit, under conditions installation and operation, without the conductors exceeding the Maximum operating temperature;
- maximum operating temperature: temperature which must not be surpassed in normal service, to ensure that the cable has a reasonable life ($\approx$ 25 years);
- cable life: the time for which the cable insulator can withstand in continuous mode a certain temperature before its electrical characteristics and especially mechanical decay in an unacceptable way;

The dimensioning of cable lines consists in determining: the section, the element conductor (Cu or Al) and the type of insulation.

The cross-section of a cable must be such that:

- I_z is not lower than the operating current I_b;
- the voltage drop across it remains within the imposed limit.

Thermal criterion

As for the thermal criterion, the Reference Standard is CEI UNEL 35024/1 which defines the maximum current that cable can transmit as:

$$I_z = I_0 \cdot k_1 \cdot k_2 \tag{41}$$

where:
I_0 is the cable capacity in conditions defined by the standard, called standard conditions;
k_1 is the corrective factor taking into account a different ambient temperature from standard ambient temperature of 30 °C. In particular, if the ambient is greater than 30 °C, then this coefficient acts as a reducing factor, if temperature is lower than 30 °C acts as an expansion factor;
k_2 is the corrective factor which takes account of the presence of multiple cables inside a conduit.

The thermal criterion for the sizing of cable lines belonging to the primary distribution, consists in deriving the capacity Iz of the cable line, which must be higher than the operating current I_b of the line itself.

Voltage Drop along Cables

Once that the thermal criterion is verified, the next step is to verify the maximum voltage drop on the line.

The standard CEI 64-8 state that: the maximum voltage drop MUST be lower than 4%. This value is intended from the PV modules to the connection

point with the grid. Supposing a voltage drop inside the transformer of $\approx 0.5\%$ it is a good practice to keep the voltage drop from PV modules to the inverter at 2% in photovoltaic generation plants.

To calculate the voltage drop along the line, the Eq.42 is used to estimate the voltage drop:

$$\Delta V\% = \frac{2 \cdot R_L \cdot I_{mpp}}{V_{mpp}} \cdot 100 \tag{42}$$

where:
R_L: $r \cdot l_{cable}$ cable line resistance;
l_{cable}: cable line length;
I_{mpp}: Current at Maximum Power;
V_{mpp}: Voltage at Maximum Power.

According to what was explained in Sec.1.3 the sizing is made only for one functional unit (e.g. 20 string in parallel to the DC combiner box, or the 13 DC combiner boxes in parallel to the inverter input) and the others functional unit will be the exact same copy.

To calculate strings to DC combiner boxes voltage drop the hypothesis stated to perform the calculations are the following:

- solar cables placed in a conduit;
- ambient temperature 70°C;
- cable insulation in HEPR G21;
- one cable per conduit;
- conductor made in copper.

Since usually it is the more strict criteria in dimensioning lets start calculating the voltage drop across the string and the piece of cable that connects the string to the DC combiner box

Impp	13,92	A
Vmpp	44,55	V
Vstring	846,45	V

Table 23: String and module's data.

Now using Eq.(42) and selecting the cable FG21M21 [18](nominal voltage 1.2 kV) the following values of voltage drop and voltage are calculated:

[18]FG21M21 solar cable

Cable FG21M21 Data	**length [m]**	**section [mm^2]**	**r [ohm/km]**	**R [ohm]**	**cable voltage [V]**	ΔV [%]
String 1	114	10	1,95	0,222	840,3	0,73
String 2	112,8	10	1,95	0,220	840,3	0,72
String 3	111,6	10	1,95	0,218	840,4	0,72
String 4	110,4	10	1,95	0,215	840,5	0,71
String 5	109,2	10	1,95	0,213	840,5	0,70
String 6	108	10	1,95	0,211	840,6	0,69
String 7	106,8	10	1,95	0,208	840,7	0,68
String 8	105,6	10	1,95	0,206	840,7	0,68
String 9	104,4	10	1,95	0,204	840,8	0,67
String 10	103,2	10	1,95	0,201	840,8	0,66
String 11	102	10	1,95	0,199	840,9	0,65
String 12	103,2	10	1,95	0,201	840,8	0,66
String 13	104,4	10	1,95	0,204	840,8	0,67
String 14	105,6	10	1,95	0,206	840,7	0,68
String 15	106,8	10	1,95	0,208	840,7	0,68
String 16	108	10	1,95	0,211	840,6	0,69
String 17	109,2	10	1,95	0,213	840,5	0,70
String 18	110,4	10	1,95	0,215	840,5	0,71
String 19	111,6	10	1,95	0,218	840,4	0,72
String 20	112,8	10	1,95	0,220	840,3	0,72

The cable length are calculated following the simplified schematic: the estimated length is higher than the actual one, since the cables will not follow straight lines but they need to have a minimum curvature radius of 3 times their diameter (24 mm for this 10 mm^2 section).

The optimal cable routing should be agreed upon between the designer and the installer. This is because the installer has practical experience with the work and can provide valuable insights into the feasibility and efficiency of the proposed solutions. Additionally, this process depends on field measurements and observations. Collaboration between these two professionals ensures that the project not only meets technical standards but is also optimized for practical and safe implementation.

This considerations suggestion will not be repeated, but stands also for the laying of all cables and conduits.
The voltage drop is slightly different on each cable due to different length of the cables, but this difference are acceptable.

After verifying the voltage drop criterion withe Eq.(41) lets verify the thermal criterion:

$$I_z = I_0 \cdot k_1 \cdot k_2 = 70 \cdot 0.522 \cdot 1 = 36.54A \tag{43}$$

k_1 and k_2 coefficients are chosen according to CEI-UNEL 35024/1 standard:

- $k_1 = 0.58 \cdot 0.9 = 0.522$ (at 70°C(0.58) and closed in a conduit (0.9))

- $k_2 = 1$ (only one conductor per conduit)

I_z is greater than $I_b(39)$ so the thermal criterion is verified.

To calculate the voltage drop from the DC combiner boxes to inverter the hypothesis stated to perform the calculations are the following:

- solar cables placed in a conduit;
- ambient temperature 30°C;
- one cable per conduit;
- conductor made in copper.

Distance between Dc combiner boxs [m]	23.67
I DC box [A]	378,5
V DC box [V]	840,3

In this section of the plant solar cables are not mandatory because they are not directly exposed to outdoor weather conditions, nevertheless they are adopted for their superior electrical characteristics.

Also in this case using Eq.(42) and selecting as a cable the "E-BEAM IRRADIATED XLPO SOLAR CABLE"[19], the following results are obtained:

[19]E-BEAM IRRADIATED XLPO SOLAR CABLE

E-BEAM IRRADIATED XLPO SOLAR CABLE	**cables length [m]**	**sezione [mm^2]**	**specific resistivity [ohm/km]**	**R [ohm]**	**cable voltage [V]**	**Δ V [%]**	**ΔP [%]**
DC combiner box 1	49,36	240	0,0817	0,00403	832,1	0,36	0,36
DC combiner box 2	25,68	240	0,0817	0,00210	833,5	0,19	0,19
DC combiner box 3	1	95	0,210	0,00021	834,8	0,02	0,02
DC combiner box 4	1	95	0,210	0,00021	832,1	0,02	0,02
DC combiner box 5	25,68	240	0,0817	0,00210	833,2	0,19	0,19
DC combiner box 6	49,36	240	0,0817	0,00403	836,7	0,36	0,36
DC combiner box 7	73,04	300	0,065	0,00478	840,2	0,43	0,43
DC combiner box 8	52,06	240	0,0817	0,00425	836,7	0,38	0,38
DC combiner box 9	28,38	240	0,0817	0,00232	833,2	0,21	0,21
DC combiner box 10	3,7	95	0,210	0,00078	832,1	0,07	0,07
DC combiner box 11	3,7	95	0,210	0,00078	834,8	0,07	0,07
DC combiner box 12	28,38	240	0,0817	0,00232	833,5	0,21	0,21
DC combiner box 13	52,06	240	0,0817	0,00425	832,1	0,38	0,38

In this case the voltage drop difference is higher, as between the maximum and the minimum there is a difference of about 0.41%; the MPPT of the inverter will regulate the voltage in order to maximize the overall energy production of the set.

The section chosen for the cables are different and are chosen to create the least differences possible between the voltage of the cables.

As seen in the previous subsection lets move forward verifying the thermal criterion, the verification will be carried out only for the smallest section (120 mm^2), since if that section will pass it also the other section will pass it.

Using the Eq.(41):

$$I_z = I_0 \cdot k_1 \cdot k2 = 464 \cdot 0.9 \cdot 0.96 \cdot 1 = 400.9A \tag{44}$$

k_1 and k_2 coefficients are chosen according to CEI-UNEL 35024/1 standard:

- k_1 =0.9 (cable closed in a conduit); 0.96 (maximum temperature of the cable 35°C);
- k_2 = 1 (only one conductor per conduit).

I_z is greater than I_b=378.5 A(40) so the thermal criterion is verified.

The connection between the inverter and the primary side of the transformer is a crucial part in the design of the plant, since the currents are extremely high (3300 A maximum current) the cable needed are very thick.

The adopted cable is the ARE4M1[20] model from Prysmiat, and each phase has 6 cables in parallel that connects the busbar of the inverter to the busbar of the transformer, each cable carries at most 550 A of current (the total current for each phase will be $6 \cdot 550 = 3300$ A).

The distance from the inverter to the transformer is very short (this is one of the strongest advantages in adopting the centralized inverter configuration).

cable length [m]	1.5
Cable Voltage [V_{ac}]	434
Cable current [A]	550
cable section [mm^2]	630
r [Ohm/km]	0.0469
R [mOhm]	0.07035
X [mOhm]	0.195
Voltage drop [V]	0.1413
Voltage drop [%]	0.03

To calculate the voltage drop from the inverter to BT/MT transformer according to CEI 64/8 the equation used is:

$$\Delta V = \sqrt{3} \cdot I \cdot [R \cdot cos(\phi) + X sin(\phi)] \approx 0.1413 \ V \tag{45}$$

In terms of perceptual voltage drop the result is given by:

$$\Delta V_{\%} = \frac{\Delta V}{V_{nom}} = \frac{0.1413}{434} = 0.03\% \tag{46}$$

In this case, the voltage drop is negligible, on the other end the thermal criterion is more challenging to meet. Using Eq.(41) I_z result:

$$I_{z,cable} = I_0 \cdot k_1 \cdot k2 = 731 \cdot 0.783 \cdot 1 = 572.37A \tag{47}$$

k_1 and k_2 coeffiecients are chosen according to CEI-UNEL 35024/1 standard:

- k_1 =0.9 (cable closed in a conduit); 0.87 (maximum temperature of the cable 45°C);

[20] ARE4M1 630 mm^2 prysmiat cable, pag.62

- $k_2 = 1$ (only one conductor per conduit).

I_z for a single phase equal to :

$$I_{z,phase} = I_{z,cable} \cdot 6 = 572.37 \cdot 6 = 3434.22A \tag{48}$$

$I_{z,phase}$ is greater than $I_{b,phase}$=3300 A so the thermal criterion is verified.

3.3 Electrical Protection Devices

The protection systems are essential for the correct operation of the plant and for the safeguard of the operators and for the devices that make up the system.

Fig.36 will be used for a schematic and visual description of where a fault or a problem can happen and where the safety device will be mounted.

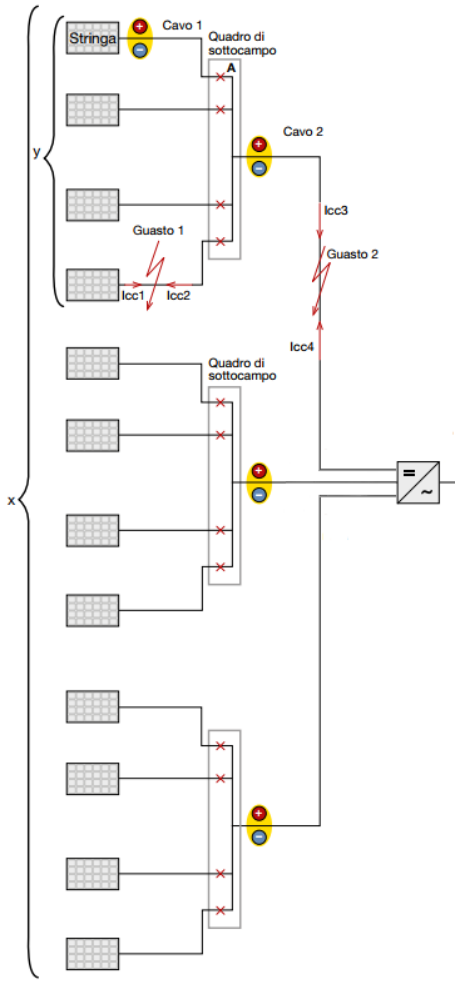

Figure 36: Simplified schematic from strings to inverter.

Where:
"Quadro di sottocampo" represents the DC combiner box;
y = 20 is the number of strings connected to the same DC combiner box ;
x = 260 is the total number of strings connected to the same inverter.

Reverse Current Protection

In the event of shading or faults, a string may become inactive, absorbing and dissipating the electrical power generated by the other strings connected in parallel to the same DC combiner box. This occurs through reverse current flowing through the affected string, opposite to its normal operating direction,

potentially causing damage to the modules that can withstand a current between 2.5 e 3 Isc (IEC TS 62257-7-1). To avoid this problem a double protection system is used:

1. A blocking diode is installed at the beginning of each string (after the last module of the latter);

2. Inside the DC combiner box there is a positive and negative fuse (bipolar fuse 20 A rated).

The blocking diodes alone are not sufficient since, as stated by the standard IEC TS 62257-7-1, the possibility that the blocking diode does not function properly and is shorted out must be taken into account. This is the reason why also the fuse is needed, if a reverse current of a value superior than 20 A flows into the fuse, it melts and block the reverse current. If this happens the string will be disconnected and and operator will replace the diode and the fuse (if the fuse melts means that the diode is not working as it should).

The downside of this protection is that a voltage drop of 0.7 V will happen on the junction of the diode and this will slightly decrease the power production of the string.

According to "guida CEI 82-25" standard, the nominal reverse voltage of the diode should be $\geq$ 2 $V_{OC,string}$ (2000 V) and with a nominal current $\geq$ 1.25$\cdot$ I_{SC} (18.925 A). The diode chosen is the OCD1D1-20A[21] produced by "OCRAM power electronics"

[21] OCD1D1-20A diode

Parameter	Description	Value
VL	Maximum voltage string (T 150°C)	1000 V
Vrrm	Repetitive peak reverse voltage (Tj 175°C)	2000 V
Vf	Forward voltage (If = 20A)	1 V
Iavg	Maximum continuous current for single diode (T 40°C)	20 A
Ifsm	Surge forward current (Tvj = 25°C; 10ms)	1150 A
I^2t	I^2t value (Tvj = 25°C; 10ms)	6600 A^2s
Tj (max)	Junction temperature	180°C
Tcase (max)	Heatsink temperature	100°C
Rth j-c	Thermal resistance junction to case	3 °C/W
Ird	Direct reverse current (max)	4 mA
Qrr	Recovered charge (Tvj = 10°C; Vrd = Vrrm)	20 µC
Tvj	Virtual junction temperature (Tvj = 160°C; di/dt = 10A/µs)	da -40°C a +180°C
Visol	Insulation test voltage (r.m.s)	6000 V
Size	Dimensions (L × W × H)	100 × 105 × 45 mm
Weight	Weight	240 g

Table 24: Blocking diode parameters.

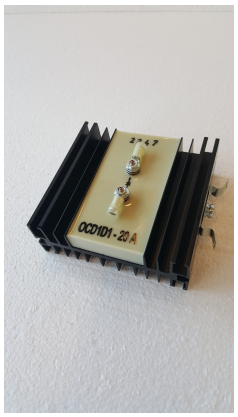

Figure 37: Blocking diode picture.

The producer of the DC combiner box gives the possibility to customize the

fuse based on the client needs, since in the datasheet of the combiner box is not clearly indicated what kind of fuse there is inside the box CH/SP 10x85 gPV FUSE has been chosen. It is a cylindrical fuses for modules string protection of photovoltaic plants.

In Tab.25 its characteristics are shown:

Parameter	Value
nominal current [A]	20
rated voltage [V]	1500
I^2t	431
breaking capacity [kA]	30
time-current characteristic	gPV
dimentions [mm]	10 x 85
Standard	IEC 60269-1, IEC 60269-6

Table 25: fuse parameters.

Figure 38: CH/SP 10x85 gPV FUSES picture.

The fuse has a fast-blow characteristic in order to protect the cables and the modules placed upstream. Since there are x strings connected in parallel to the inverter the maximum reverse current will be:

$$I_{rev} = (x-1) \cdot 1,25 \cdot I_{SC} = (260-1) \cdot 1,25 \cdot 15,14 = 4901.58\ A \qquad (49)$$

I_{rev} is so high that the fuses acts in µs, but is lower than the breaking capacity of the fuse, so it will be able to safely interrupt the current.

Load-Break Disconnector

Embedded in the DC combiner box there is a load-break disconnector that allows:

- Switching operations (opening/closing) of a circuit under nominal load conditions;
- Ensuring safe disconnection (isolation), when it is open the strings connected in parallel to the DC combiner are separated from the inverter, allowing maintenance work.

Fault and Short-Circuit Protection

Regarding short circuits, the DC-side cables are affected by such over-current in the case of:

- Fault between the polarities of the photovoltaic system;
- Ground fault in grounded systems;
- Double ground fault in isolated (ungrounded) systems.

Two main scenarios will be analyzed: a short circuit on a string cable (indicated as "guasto 1" in Fig.36) and a short circuit between a combiner box and the inverter (indicated as "guasto 2" in Fig.36). In the first scenario, we consider a short circuit on a cable connecting a string to a combiner box ("Guasto 1"). This short circuit is fed both upstream by the affected string, with a current

$$I_{cc1} = 1.25 \cdot I_{sc} = 1.25 \cdot 15.14 = 18.925A \tag{50}$$

and downstream by all the other (x-1) strings connected to the same inverter[22], with a current

$$I_{cc2} = (x-1) \cdot 1.25 \cdot I_{sc} = 259 \cdot 1.25 \cdot 15.14 = 4901.58A \tag{51}$$

If the system is larger and has three or more strings (x $\geq$ 3), the current I_{cc2} exceeds the operating current. Therefore, it is necessary to protect the string cables from short circuits since their current-carrying capacity $I_z \leq I_{cc2}$, i.e., if $I_z < (x-1) \cdot 1.25 \cdot I_{sc}$. In the second scenario, we examine a short circuit between a combiner box and the inverter ("Guasto 2"). This short circuit is fed upstream by the y parallel strings in the subfield, with a current

$$I_{cc3} = y \cdot 1.25 \cdot I_{sc} = 20 \cdot 1.25 \cdot 15.14 = 378.5A \tag{52}$$

and downstream by the remaining (x-y) strings connected to the same inverter, with a current

$$I_{cc4} = (x-y) \cdot 1.25 \cdot I_{sc} = (260-20) \cdot 1.25 \cdot 15.14 = 4542A \tag{53}$$

The current I_{cc3} coincides with the operating current of the circuit between the subfield combiner box and the inverter. However, the current (I_{cc4}) exceeds the operating current if (x-y > y as in our case). In this case, it is necessary to

[22]Inverter short circuit current is 6400 A and can't be reached with this configuration.

protect the cable from short circuits if its current-carrying capacity I_z is less than I_{cc4}. The latter conditions happens for all cables (even the thickest one with section 300 mm^2). For protection against short circuits on the DC side, the devices used must be suitable for DC applications and have a rated nominal voltage V_{nom} greater than the maximum generator voltage, which following standard IEC TS 62257-7-1 is:

$$V_{nom} = 1.2 \cdot V_{oc} = 1.2 \cdot 1064.95 = 1277.94V \tag{54}$$

Additionally, the protective devices must be installed at the end of the circuit to be protected, starting from the strings and moving toward the inverter. This positioning is critical because the short-circuit currents originate from the other strings (from downstream rather than upstream) as specified in IEC TS 62257-7-1. All the components (except the DC combiner on which there are no information available concerning this security issue) are protected against double failure so the idea is to install an automatic switch at the end of the cable that connects the DC combiner to the inverter. In this way, the cable is protected and the maximum I_{CC2} drops to $\approx$ 360 A since it can be fed only by the other 19 strings of one combiner box. Despite the fault occurrence is extremely unlikely, even if there is a fault in the section between the string and the inverter the diode and the fuse will protect the modules. The switch selected is OTDC400FV11[23] from ABB, a fully optimized two-pole DC switch-disconnector for 1500V utility-scale photovoltaic power plants covering 400 A. The new design offers both a size reduction and an increase in efficiency and performance to help manufacturers adapt to the industry's rapid adoption of 1500V DC solutions. Measuring just 150mm wide and 122mm high, the OTDC range of 1500V DC switches is also up to 30 percent smaller than conventional solutions. Main characteristics for this particular OTDC type are shown in Tab.26:

Parameter	**Value**
nominal current [A]	400
rated voltage [V]	1500
breaking capacity 1500 V$_{DC}$[kA]	10
dimentions [mm]	157.5x211x135
Standard	IEC 60947-1,-3
connection	lug terminals
number of poles	2

Table 26: OTDC400FV11 DC switch ABB.

To prevent untimely tripping during normal operating conditions, the switch installed has a rated nominal current (I_n) that satisfies the following condition:

$$I_n \geq 1.25 \cdot I_{sc} \cdot y \geq 378.5A$$

[23]OTDC400FV11 DC switch ABB.

where:
I_n is the rated nominal current of the switch device,
I_{sc} is the short-circuit current of the string.
y is the number of string connected in parallel
This ensures that the protective devices operate correctly under fault conditions without unnecessary interruptions avoiding false tripping during normal operation.

Surge Protection and Lightning Mitigation

In the plant there is one SPD (type 1+2, class I+II) for each combiner box that is responsible for the protection of the DC side and one SPD for each inverter that is responsible for the protection on the AC side (type 1+2, Lightning Protection Level III up to 100 kA) Surge Protection Devices (SPDs from now on) are protective devices that avoid damage to modules, electronic and electrical equipment if an overvoltage occurs. These overvoltages can be generated by lightning strikes, switching operations on the electrical grid, or electromagnetic disturbance. First of all they need to sense the eventual overvoltage, then they dissipate the extra energy to the ground thanks to components such as Metal Oxide Varistors (MOV) or Transient Voltage Suppressors (TVS), after this they return to their initial state ready to manage new overvoltage events.

SPDs are divided in three types:

1. type 1: protect from direct ligthing strikes;
2. type 2: protect from internal overvoltage, like the one generated from switching operations;
3. type 3: protect the more sensible devices and are installed next to the electrical loads.

3.4 Grid Connection and Compliance with Standards

In Italy the rules for the connection to the MV and HV grid are given from the CEI-016 standard:"Reference technical rules for the connection of active and passive consumers to the HV and MV electrical networks of distribution Company".

The edition used in this thesis is the 2019-04 version that is a consolidated version of CEI 0-16:2014-09 itself, the Variant V1:2014-12, of Variant V2:2016-07 and of Variant V3:2017-07. The new features of this new edition concern alignment with the requirements of EU Regulation 2016/631, the EU Regulation 2016/1388 and EU Regulation 2016/1447. In particular, the major changes have have been induced by the transposition of EU Regulation 2016/631 (Requirements for Generators - RfG), which has involved the division of generators into 4 distinct classes, based on the size and voltage of the point of connection:

- Type A: power equal to or greater than 800 W and less than or equal to 11.08 kW;

- Type B: power greater than 11.08 kW and less than or equal to 6 MW;
- Type C: power greater than 6 MW and less than or equal to 10 MW;
- Type D: power greater than or equal to 10 MW or connection point voltage greater than or equal to 110 kV.

This Standard completely replaces IEC 0-16:2014-09 and its Variants. The generation plant designed falls under category C.

The CEI 0-16 standard describe 6 possible connection schemes. Regardless of the chosen connection solution, the user-side network system always reflects the configuration shown in Fig.39. Starting from the MV cable downstream of the connection point, the figure illustrates the user's installation scheme for the connection.

The Distributor's substation at the user's premises is the one built to connect the User's system. The arrangement of the measuring devices refers to the general case of a passive User; in the case of active Users, if the measurement devices are owned by the User (injection point), they must be positioned immediately downstream of the main device, in a location that ensures they are protected (against fault currents from the grid) by the main device itself.

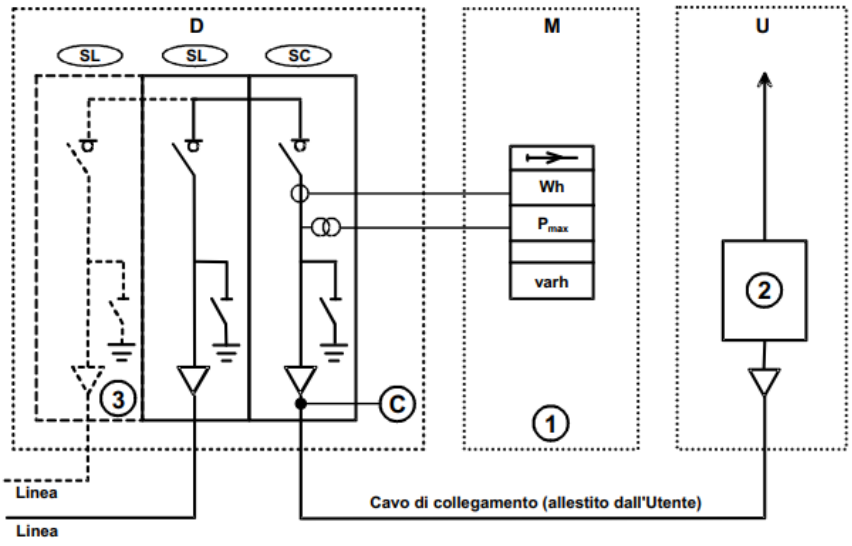

Figure 39: Connection diagram between the Distributor's substation at the user's premises and the system configured as a withdrawal point[7].

Legend:
D = Distributor's premises at the user's site
M = Room for metering
U = User's room

SL = Line compartment cell
SC = Delivery compartment/cell
C = Connection point
1 = Metering group
2 = User's general device
3 = Compartment for in-out connection, existing or to be planned

Table 27: Solutions for connection to distribution grid MT.

			D	B2	C	A	B1
Active Users	**Nominal power MW**	**Rete**	**Derivazione a T**	**Antenna su CS**	**Antenna su CS in derivazione**	**Entra-Esce**	**Antenna su CP**
	0,1 - 0,2	BT	Nc	nc	nc	nc	nc
		MT	X$^{(1)}$	X	X	X	-
	0,2 - 1	MT	-	X	X	X	X
	1 - 3	MT	-	-	-	X	X
	3 - 6	MT	-	-	-	-	X
	6 - 10	MT	-	-	-	-	X
		AT	Nc	nc	nc	nc	nc

Legenda

- X: suggested solution;
- $\chi^{(1)}$: viable solution but not recommended;
- -: not recommended solution;
- nc: case not considered in this table.

In Tab.27 for generation plants in the power range 6-10 MW is suggested the Connection **"Antenna su CP"** according to CEI 0-16 standard.

The connection "Antenna su CP" refers to a specific configuration for connecting power generation plants to the medium voltage (MV) distribution network.

Description of the "Antenna su CP" Connection:

"CP" stands for "Primary Substation", which is a transformation substation that connects the high voltage (HV) network to the medium voltage (MV) network. In this kind of connection the power generation plant (a photovoltaic generator in our case) is directly connected to the primary substation through a dedicated line ("antenna"). This type of connection is typically used for medium-to-large power plants (above 1 MW), as it requires a direct and dedicated line to the primary substation.

It requires more complex and costly infrastructure compared to other connection solutions, such as a T-connection or an "Antenna su CS" (Secondary Substation). but offers greater stability and control over the connection.

Usually the primary substation should be within a 10 km range from the plant.

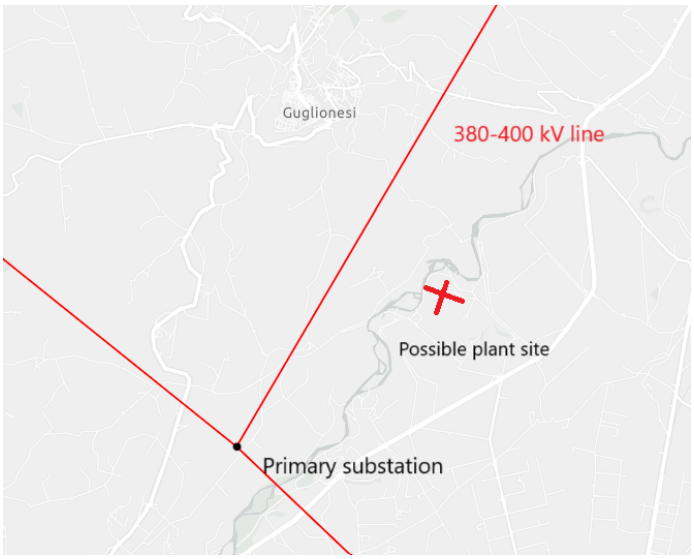

Figure 40: Distance between plant and primary substation[8].

In Fig.40 is showed the distance between the possible plant site and the closest primary substation, it should be around 1.5 km.

Metering and General Circuit Breaker Requirements

In Fig.41 the User general device (2 in Fig.39) is expanded, this two schematics represents the guidelines that every production unit (PV array, inverter, transformer etc.) must follow.

It is the responsibility of the designer to size the distribution transformer and the general device[24]connected to it, whereas the measurement room is usually designed by the designer with the supervision of the distributor to ensure a correct measurement of the energy withdrawn/injection into the grid.

[24]Indicated as: "DG DISPOSITIVO GENERALE" in Fig.41.

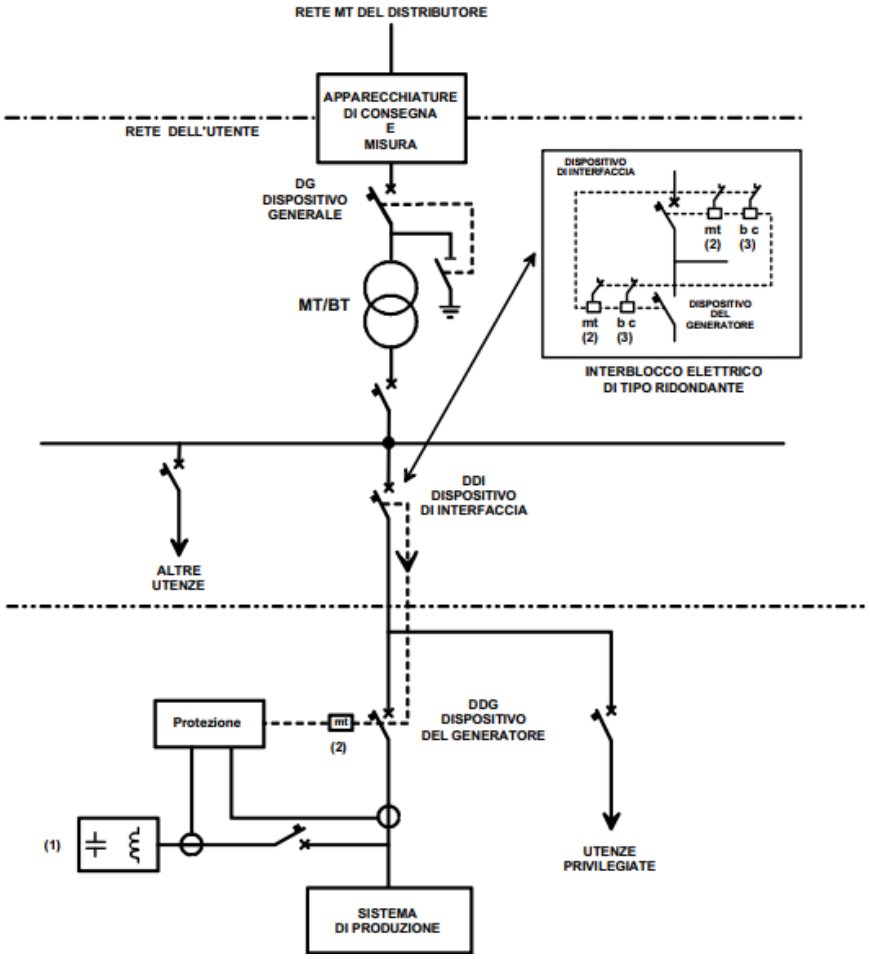

Figure 41: Wiring and protection scheme for standalone power generation systems with electrical and mechanical interlocking or with redundant electrical interlocking[7].

Before the room for metering there is the general circuit breaker from the user side, it is an automatic circuit breaker usually using SF_6 (sulfur hexafloride) or vacuum technology, as these ensure high reliability and safety in medium voltage applications. It can be installed in an air-insulated switchgear (AIS) or a gas-insulated switchgear (GIS), depending on the specific requirements of the installation.

To size this circuit breaker the DSO should provide the value of the short-circuit power of the grid. A value of S_{sc}= 500 MVA can be assumed[25]. For a

[25]Since if we want the correct value we should contact the DSO and do all the paperwork.

three-phase fault, the short-circuit current I_{sc} can be calculated as:

$$I_{\text{cc}} = \frac{S_{\text{cc}}}{\sqrt{3} \cdot V_{\text{nom}}} = \frac{500 \cdot 10^6}{\sqrt{3} \cdot 20 \cdot 10^3} = 14434A \tag{55}$$

Where:

- I_{cc} = three-phase short-circuit current (A)
- S_{cc} = short-circuit power of the grid at the point of connection (VA)
- V_{nom} = nominal voltage of the grid (V)

This formula assumes a three-phase fault without additional impedances along the line.

Furthermore a the circuit breaker have to withstand a voltage value of 24 kV (if the MV line is a 20 kV rated line).

The nominal current that the circuit-breaker has to withstand is calculated with:

$$I_n = \frac{S_{trans}}{\sqrt{3} \cdot V_n} = \frac{2.5 \cdot 10^6}{\sqrt{3} \cdot 20^3} = 71.2A \tag{56}$$

and is also the nominal value of current that flows through the MV cable.

The measuring transformers must have suitable design characteristics in relation to the type of installation and the operating voltage of the network at the connection point. For networks with voltage levels between 15 and 20 kV, the following minimum insulation values are recommended:

- Maximum reference voltage for insulation: 24 kV, the same of the BT/MT transformer;
- Industrial frequency withstand voltage (50 Hz): 50 kV;
- Accuracy class: must be equal to or better than 0.5
- Atmospheric impulse withstand voltage: 125 kV.

The rated performance (VA) of transformers must be compatible with the impedance of the circuit connected downstream of the secondary. Current transformers must also have the following technical characteristics (recommended by the DSO of the site "E-distribuzione"):
- rated thermal dc current for 1 second 12.5 kA;
- dynamic rated current 31.5 kA;
- safety factor 15;
- rated permanent thermal current between 1 and 2 times the maximum current flowing at the connection point.

Standards Utilized

- **IEC 60947-3** – Low-voltage switch-disconnectors, isolators, and fuse-combination units.
- **IEC 61439-2** – Low-voltage switchgear and controlgear assemblies: requirements for assembled structures.
- **CEI 0-16** – Connection regulations for active and passive users to the MV and HV distribution network.
- **CEI UNEL 35024-1** – Thermal correction factors k_1 and k_2 for cable sizing.
- **CEI 64-8** – Voltage drop limits in electrical installations.
- **CEI EN 60228 (CEI 20-29)** – Electrical resistance and conductor classification for cables.
- **CEI 82-25 Guide** – Nominal voltage selection criteria for fuses in photovoltaic systems.
- **IEC TS 62257-7-1** – Use of blocking diodes and overcurrent protection requirements in PV modules.
- **IEC 62305-1** – Protection against lightning: general principles.
- **CEI EN 61000-3-6** – Electromagnetic compatibility (EMC): limits for voltage fluctuations and harmonic emissions in MV and HV networks.

4 Electricity Market Framework, Economic and Environmental Considerations

4.1 Elecrticity Market Structure

In the year 2000 with the "Decreto legislativo 79/99" the GME "Gestore Mercati Elettrici", Its mission is to: organize and manage the transaction in the electricity market under criteria of neutrality, transparency objectivity and competition between producers. GSE together with "Acquirente Unico" (AU) and "Ricerca sul sistema energetico" (RSE), are placesd under the supervison of "Gestore dei Servizi Elettrici" that as head of the group, exercise its guidance and coordination functions over this Companies, all of which operate in the energy field and have a public purpose.

In turn GSE is owned by the Ministery of Economy and Finance and started its operation in March 31st, 2004.

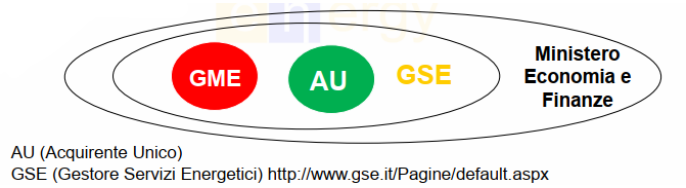

Figure 42: GSE structure[9].

The "Decree 79/1999" sanctioned the separation between ownership and management of the national transmission grid. Two new companies are established: Terna, owner of the Italian transmission grid, and GRTN (the National Transmission Grid Operator). Before 2005: GRTN (Gestore Della Rete Di Trasmissione Nazional) dealt with the management of electricity transmission and dispatching activities.

The market is composed by *Sellers*: generation companies or brokers entitled to sell electricity on the market, and *Eligible buyers*: consumers and brookers entitle to buy power on the market (they are only large buyer). The small buyers are called *Not eligible buyers* and they can only buy electrical energy by energy dealers.

The operators (sellers, eligible buyers) submit offers (bids) to sale (buy) electricity that are related to the injection (withdrawal) points.

The offer/bid points injection/withdrawal point can be of mixed type: both injection/withdrawal can be at the same point for example hydroelectric power plant with pumping station, but also the other power plants have to declare their maximum injection/withdrawn to the DSO/TSO.

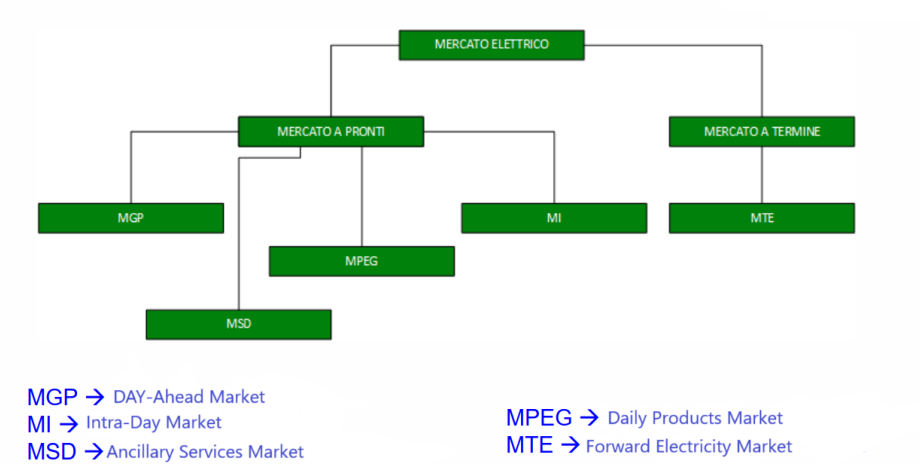

Figure 43: Electricity Markets.

In Fig.43 There is a schematic of the different markets, the first fork is between:

- Spot Electricity Market ("Mercato elettrico a pronti - MPE"): enables producers, consumers and wholesale customers to enter into the electricity purchase and sale for the next day;
- Forward Electricity Market ("Mercato elettrico a termine – MTE"): where participants may sell/purchase future electricity supplies.

In GME's Spot Electricity Market (MPE), four types of offers/bids may be submitted:

- Simple: constituted by a couple of values (quantity/ unit price) reported to a point of offer, to a market and to a relevant period (day, month or year -presentable offer to the MGP, MI and MSD);
- Multiple: constituted by series of simple (max four couples quantity/ unit price) offers introduced by the same operator for the same relevant period, reported to only one point of offer (can be submitted only to MGP and MI);
- Balanced: sale offers with void price and purchase offers without price indication related to the same relevant period and belonging to points of offer of the same geographical zone or pole of production limited, with balanced quantities and specifically identified in their combination sale/purchase (special alphanumeric code chosen by the operators);
- Default: simple or multiple offers, considered as proposed by an operator in every session of the MGP in which the GME doesn't receive offers from the operator himself (offered presentable only on the MGP and on the MSD).

Day-Ahead Market (MGP)

The market opens at 8 AM of the ninth day before the day of delivery and closes at 12 PM of the day before the day of delivery. the TSO provide some preliminary information such as hourly energy demand, CIP6 programs and network constraints.

The bids are expressed in price-quantity couples specifying the quantity and the minimum (maximum) price at which seller (buyers) are willing to sell/purchase.

The Clearing mechanism order offers/bids under the economic merit order criterion, taking into account transmission constraints between zones. The supply side is remunerated following the zonal prices (of the zone which they belong), while demand side pays the National Single Price ("PUN - Prezzo Unico Nazionale") that is calculated as weigthed average zonal price, weighted on zonal consumption, this is known as "Pay as Clear" mechanism.

Infra-Day market

The input information of the market is the notification of the results of MGP, it opens at 10:30 AM and closes at 2:00 PM the bids/offers and market clearing mechanism are the same of the MGP.

both offers and bids are paid the zonal price (that is equal to the PUN if there is no congestion into the grid.

Ancillary Services Mmrket (MSD)

This market follow a "Pay as Bid" mechanism, this means that offers/bids are valued at the offered price. Is divided in six sessions: MSD1, MSD2, MSD3, MSD4, MSD5 and MSD6.

Daily Products Market (MPEG)

The Daily Products Market (MPEG) is a flexible and inclusive trading mechanism designed to facilitate the exchange of daily energy products in the electricity market. It admits automatically all participants in the electricity market, the trades within the MPEG take place in continuous mode, allowing participants to engage in transactions throughout the trading session without interruptions.

The GME plays a central role in this market, acting as the general counterparty for all transactions.

The MPEG supports trading of daily products under two distinct pricing mechanisms:

- "Unit price differential": price corresponds to the differential expression (compared to the PUN), to which participants are willing to trade such products;
- "Full unit price": In this case, the price corresponds to the absolute unit value of the electricity exchange specified in the traded contracts.

Both pricing mechanisms allow for the negotiation of Base-load and Peak Load products, providing participants with flexibility to meet their specific energy needs. Furthermore, the net electricity delivery position resulting from daily product trades in the MPEG is recorded in corresponding transactions within the PCE, ensuring accurate tracking and settlement of energy exchanges.

Forward Electricity Market

In this market there is also another mechanism of bid/offer called: "Bilateral Contract". It is defined between seller and buyer without passing by the mediation of power exchange platform or GME, the buyer add the seller are not obliged to declare the price, but they need to declare the quantiy of energy injected/withdrawn from the grid and thei respective points in order to let the TSO and DSO manage the grid in the best possible way.

According to the AEEG's Decision 111/06 bilateral transactions are to be registered into the Registration Platform ("Piattaforma Conti Energia -PCE").

Returning to Fig.43 on the right side of the first fork there is the Forward Electricity Market (MTE - Mercato Elettrico a Termine), that is the venue where forward electricity contracts with delivery and withdrawal obligation are negotiated. The MGP/MI participants are automatically admitted to the MTE, the trade window of MTE is always open. The possible contracts are: "Base-Load" and "Peak-Load", with weekly and monthly delivery periods. Market Participants submit orders where they specify the type and period of delivery of contracts, the number of contracts and the price at which they are willing to purchase/sell, as well as the forward electricity accounts on the PCE[26] to which the transactions are be referred in case of matching of the orders .

For the Electricity Market (MPE and MTE) there are some fees utilized from GSE and GME to pay their employees and to improve the service:

- Access fee (one-time): €7500;
- Yearly fixed fee: €10000;

For the MPE, a regressive variable fee is defined as follows:

- Initial exemption on the first 0.02 TWh of monthly traded electricity;
- Fee of 0.04 €/MWh for monthly traded electricity volumes exceeding the threshold of 0.02 TWh, up to a maximum of 1 TWh;
- Fee of 0.03 €/MWh for monthly traded electricity volumes exceeding the 1 TWh threshold, up to a maximum of 10 TWh;
- Fee of 0.02 €/MWh for monthly traded electricity volumes exceeding 10 TWh.

Since the production of the plant never exceed the 0.02 TWh monthly limit the total expenditure derived from the fees can be estimated with:

$$C_{fees} = C_{access} + n \cdot C_{yearly} = 7500 + 25 \cdot 10000 = 257500 \; Euros \qquad (57)$$

Congestion Management

The GME uses a simplified representation of the power network that divide the transmission Italian grid 7 geographic zones (North, South, middle-North, middle-South, Sicily, Sardinia, Calabria) and 6 foreign virtual zones (France, Switzerland, Austria, Slovenia, Corsica, Greece). Terna provides to GME the hourly needs and the transmission grid limits to guarantee the stability of the system.

[26]PCE is the platform through which the operators that has concluded contracts to outside of the offer system (i.e. bilateral contracts) record the obligations trade and declare the relative programs of injection and withdrawal that are engaged to execute within contracted sayings.

Figure 44: Italy zonal division[10].

Geographical Zone	Regions
North (NORD)	Aosta Valley, Piedmont, Liguria, Lombardy, Trentino, Veneto, Friuli Venezia Giulia, Emilia Romagna
Central North (CNOR)	Tuscany, Umbria, Marche
Central South (CSUD)	Campania, Lazio, Abruzzo
South (SUD)	Molise, Puglia, Basilicata, Calabria
Sicily (SICI)	Sicily
Sardinia (SARD)	Sardinia

For each hour, the PUN (Single National Price) is the weighted average of the Geographic Zonal Prices, where the weight is the consumed quantity:

$$PUN = \frac{\sum_i (P_i \cdot \nu_i)}{\sum_i P_i} \tag{58}$$

where:

- i = referring zone;
- P_i = Bought Quantity in zone i;
- ν_i = Zonal Price in zone i.

Note: If there is no zonal congestion, there is only one zonal price, which coincides with the PUN.

The result of the IPEX (Italian Power Exchange) published on the GME website reveal the market results, the main informations are:

- Volumes;
- Prices;
- Transits;
- Additional demand bids and supply offers.

4.2 Levelized Cost of Electricity (LCOE) and Amortization Schedule

There are different ways to calculate costs in the renewable energy sector, each providing unique insights. Key cost components include the expenses associated with equipment (such as photovoltaic panels or wind turbines), capital financing, total system installation, operational and maintenance costs, fuel expenditures (if applicable).

The analysis of the costs can be very detailed and can follow all the market bid/offers system, but for a first comparison between different technologies a simplified approach that considers only the core cost metrics for which reliable and widespread data are available will be used. The interest point of view for this project is to estimate the costs of investment for a private investor (that could be also a state-owned company o a prosumer[27]). To keep the analysis fair: the data should not consider government incentives, and system costs due to the high penetration of renewable are excluded.

Depending on the renewable energy supply, capital and operating expenses, and the technology's efficiency and performance, the LCOE of renewable energy technologies varies by technology, nation, and project. A discounted cash flow (DCF) analysis serves as the foundation for the methodology employed.

The time value of money is taken into account when discounting financial flows (annual, quarterly, or monthly) to a common foundation in order to determine the cost of renewable energy technology. The WACC (Weighted average cost of capital) used to assess the project, also known as the discount rate, has a significant influence on the LCOE because most renewable power production technologies are capital-intensive and fuel costs are low or as in the case of a solar or wind plant are zero.

The LCOE represents the per-unit cost of electricity generated by an energy system over its lifetime.

It is expressed as:

$$LCOE = \frac{\sum_{t=0}^{N} \frac{I_t + O_t + M_t + F_t + C_t}{(1+r)^t}}{\sum_{t=0}^{N} \frac{E_t}{(1+r)^t}} = 41.68 \text{ €}/MWh \tag{59}$$

[27] is a consumer that posses some generation capacity and can measure and inject energy into the electrical grid.

where:

- I_t represents the capital expenditures in a year t;
- O_t corresponds to operational costs in a year t;
- M_t denotes maintenance costs in a year t;
- C_t reflects other associated costs;
- E_t is the electricity generated in year t;
- r is the discount rate[28];
- N is the system's operational lifetime.

The final value was found under this assumptions:

- the capital expenditure (or CAPEX) is estimated in a total of milion € 8.93 of which 6.93 million deriving from: modules, inverters,racking and mounting, grid connection, cabling/wiring, safety and security, monitoring and control, financing costs, system design, customer acquisition, mechanical installation electrical installation.

  And the remaining part 2 million due to works for connection to the substation, feasibility study from DSO, fees of DSO, shipping and transportation costs of all components, possible minor component replacement costs.
- the operational cost is estimated in € 34650 per year;
- the maintenance cost is estimated in € 34650 per year;
- associated costs are set to zero;
- the yearly electricity generated[29] is the one found in 2.5;
- the discount rate r is assumed 6% as suggested in [5] for Europe;
- the system operational lifetime is 25 years.

The data about the costs are extracted from report [5]. The LCOE found is a competitive value for the plant size and technology, but it is a metric used mainly to compare the cost with other plants.

[28] assumed constant.

[29] Since different of energy production is modest the average value of produced energy is taken as a reference

Amortization schedule

This section presents the economic analysis of a 9.9 MVA photovoltaic plant, considering an operational period of 25 years. The key economic parameters are:

- Average annual sold energy: 18145 MWh;
- Average annual revenue: €1.74 million;
- Initial loan: €8.93 million, to cover the CAPEX costs;
- CAPEX: €8.93 million;
- OPEX: €69,300 per year;
- Loan interest rate (discount reate): 6%.

In the Italian amortization method, the repaid capital portion remains constant over time, while the interest payments decrease. In this case, the amortization percentage after n payments is given by:

$$\% \text{ Amortization} = \frac{n}{N} \times 100 \tag{60}$$

where:

- n is the number of payments made,
- N is the total number of payments.

Since the capital is repaid in equal parts, the amortization percentage increases linearly over time.

The interest paid each year is computed as:

$$I_t = R_{t-1} \cdot r \tag{61}$$

where R_{t-1} is the remaining loan principal from the previous year.

The profit is considered constant during the life of the plant and is calculated as the hourly cost of energy during year 2024[30] multiplied for the correspondent energy production of that hour, then the total is divided for 19 years to get the average annual profit.

The Net profit for each year is calculated as:

$$NetProfit = -Loan\ principal - interest - OPEX + Profit \tag{62}$$

In Tab.28 the outcome of the analysis are presented, except for OPEX that is expressed in €the other economical metrics (e.g. Loan Principal, Interest, Profit, Net profit) are expressed in millions €

[30]Data from GME website, the cost of energy for the future years are supposed the same of 2024.

Year	Average sold energy [MWh]	Loan principal	Interset (6%)	OPEX [€]	Profit	Net profit	% amortized
1	4338	8,93	0,54	69300	1,74	-9,00	14%
2	4338	7,73	0,46	69300	1,74	-7,80	27%
3	4338	6,45	0,39	69300	1,74	-6,52	41%
4	4338	5,10	0,31	69300	1,74	-5,17	55%
5	4338	3,66	0,22	69300	1,74	-3,73	68%
6	4338	2,14	0,13	69300	1,74	-2,21	82%
7	4338	0,53	0,03	69300	1,74	-0,54	96%
8	4338	0	0	69300	1,74	1,13	110%
9	4338	0	0	69300	1,74	2,80	123%
10	4338	0	0	69300	1,74	4,47	137%
11	4338	0	0	69300	1,74	6,14	151%
12	4338	0	0	69300	1,74	7,81	164%
13	4338	0	0	69300	1,74	9,48	178%
14	4338	0	0	69300	1,74	11,15	192%
15	4338	0	0	69300	1,74	12,83	205%
16	4338	0	0	69300	1,74	14,50	219%
17	4338	0	0	69300	1,74	16,17	233%
18	4338	0	0	69300	1,74	17,84	246%
19	4338	0	0	69300	1,74	19,51	260%
20	4338	0	0	69300	1,74	21,18	274%
21	4338	0	0	69300	1,74	22,85	288%
22	4338	0	0	69300	1,74	24,52	301%
23	4338	0	0	69300	1,74	26,19	315%
24	4338	0	0	69300	1,74	27,86	329%
25	4338	0	0	69300	1,74	29,53	342%

Table 28: Amortization schedule.

From the analysis emerge that the plant should have a pay-back time of approximately 7.3 years, and with an initial investment of about 9 millions €the Net profit earned in 25 years should be about 29.53 millions €.

4.3 Environmental Impact Assessment of Large-Scale PV Plants

Photovoltaic energy production is characterized by produce energy from an inexhaustible source, the sun. This characteristic allows a PV plant to produce energy without burning any kind of fuel so there are not GHGs (Greenhouse gases) emissions directly correlated with the enregy production phase.

Other advantages of photovoltaic plants respect other energy sources are:

- Reduction of the fossil fuels based-generation in the electrical power system;

- no air pollutant (e.g. NOx, SOx) associated with the production of energy;
- low waste production during its operation.

However, also the photovoltaic technology has its so environmental impacts for example: land use, water use, cells life cycle, are negative externalities that must be taken in consideration to have a complete picture of this technology.

Land Use

The plant designed should cover a surface of about 0.12 km^2. To minimize the land use modules made of mono-crystalline silicon have been used. Even considering that the PV arrays will have an important visual impact and could raise concerns about degradation of the land and habitat loss.

Water Use

Solar PV systems do not use water for energy generation but as in all fabrication process water is used. In addition, water will be required for cleaning the dust of the PV panels. But this water remains uncontaminated and can return to the water cycle without any treatment.

Hazardous Materials

PV cell manufacturing requires the use of some hazardous materials mostly used to purify and clean the semiconductor surface. These compounds includes hydrochloric acid, sulfuric acid, nitric acid, hydrogen fluoride, and acetone. The type and quantity required of these chemicals depend on the type of the cell and the size of the silicon wafer.

GHGs life cycle assessment

The Italian emission GHGs emission per kWh generated of 2024 according to electricity map[27] is about 274 $gCO_{2,eq}$/kWh, while the China emission GHGs per kWh generated[27] in 2024 is 534 $gCO_{2,eq}$/kWh

To have a perfect estimate of the reduction of $CO_{2,eq}$ we should consider the LCA (life cycle assessment) of all the components of the photovoltaic system, since this approach would be very complex, in this analysis we will consider only the LCA of the modules that are the most significant contribute.

The reason for which the life cycle of modules produce $CO_{2,eq}$ are mainly the excavation phase of the raw materials needed to make them energy efficient and the phase of purification of silicon up to solar grade silicon (10^-7 to 10^-9 defects concentration) that takes up to 65 kWh/kg.

Rare earth elements is limited compared to other sectors such as electronics or batteries. However, some elements are employed to enhance performance and efficiency.

The most commonly used rare earth elements in solar panels are:

- Europium (Eu): used in anti-reflective coatings to improve light transmission through the module glass;
- Neodymium (Nd): used in solar glass to filter specific wavelengths and reduce light loss;
- Cerium (Ce): found in some solar glass coatings to absorb UV radiation and prevent material degradation.

Considering the current China energy mix and the quantity of energy needed to produce 1 kg of solar grade silicon is possible to calculate the $CO_{2,eq}$ per produced module.

Before doing this is necessary to estimate the quantity of silicon in a module, a typical module of 33.5 kg (like the one used) is composed by:

- Glass (70% of the mass) = 23.45 kg;
- aluminum frame (12.5%) = 4.19 kg;
- crystal silicon (7.5%) = 2.513 kg
- EVA, back-sheet and other components (10%) = 3.35 kg

$$m_{SG,silicon} = Num\ modules \cdot 2.513 = 4 \cdot 260 \cdot 19 \cdot 2.513 = 49656.9\ kg \quad (63)$$

The total energy used to produce 49659.9 kg of solar grade silicon is:

$$E = m_{SG,silicon} \cdot 2\ \frac{kWh}{kg} = 12.41\ GWh \quad (64)$$

The total emission $CO_{2,eq}$ emission is[31]:

$$CO_{2,eq,tot} = E \cdot 534\,\mathrm{gCO_{2,eq}/kWh} = 6627 \cdot 10^3\,\mathrm{kg} \quad (65)$$

Now is possible, known the total energy production during their operative life (25 years), to estimate the $\mathrm{gCO_{2,eq}/kWh}$ emitted by the modules using:

$$Emission\ factor_{PV,plant} = \frac{CO_{2,eq,tot}}{total\ energy\ production} = \frac{6627 \cdot 10^6}{4.48 \cdot 10^8} = 14.8\ gCO_{2,eq}/\mathrm{kWh} \quad (66)$$

Since the carbon intensity value is lower that the current Italian mix the avoided GHGs emission are:

$$\Delta gCO_{2,eq} = total\ energy\ production \cdot (\ Emission\ factor_{Italy,mix} - Emission\ factor_{PV,plant}\ ) \quad (67)$$

the total avoided GHG emission is 31.4 kt (kilo tonnes), this is a good result that partially consider the LCA of the module.

[31] 534 $\mathrm{gCO_{2,eq}/kWh}$ is the emission factor of China where the modules are manifactured

4.4 Conclusions

The transition to carbon neutrality by 2050 is a central goal of Italian energy policy. A key strategy to achieve this objective is the decarbonization of the electricity sector, which currently accounts for approximately 32% of total greenhouse gas (GHG) emissions [13]. In this context, photovoltaic (PV) generation must at least double to meet national targets.

This thesis presents the design and techno-economic optimization of a large-scale photovoltaic-based generation plant. The proposed system is structured around a modular unit of 2.475 MVA, which can be up-scaled depending on environmental conditions and grid constraints at the selected site.

The study begins with a comparative analysis of PV module technologies, leading to the selection of monocrystalline silicon modules due to their superior efficiency and reliability. The current-voltage (I-V) characteristics of the module are modeled using manufacturer-provided datasheet parameters and a well-established exponential model based on two parameters. Following this, a comparative assessment of inverter topologies is conducted, resulting in the selection of a central inverter architecture coupled with a properly sized step-up transformer.

The system design phase determines the optimal number of modules per string and strings per inverter. This is achieved by ensuring that the string voltage remains within the inverter's operational range, considering temperature variations. The maximum number of parallel strings per inverter is determined by dividing the maximum DC input current of the inverter by the maximum string current at the highest operating temperature. Similarly, the minimum number of parallel strings is estimated by dividing the preliminary DC input power of the array by the power of a single module and the number of modules per string.

To evaluate the plant's performance, three different energy yield estimation methods are implemented:

Performance Ratio based estimation, PVGIS simulations, and an experimental hourly energy simulation.

The last model is designed for taking into account overproduction of the plant during peak production hours and analyze the energy curtailment. It is based on a meta-analysis and uses equations that relate the meteorological conditions with the output power of the modules. The meteorological data are taken from PVGIS database and cover the period from 2005 to 2023. Several assumptions are made to quantify the system's inefficiencies accurately. The hourly simulation results are further used to analyze the inverter's load profile and to estimate the energy injected into the grid over the plant's operational lifetime.

The thesis also addresses practical implementation challenges, including:

Optimal array spacing, Cable sizing, considering voltage drop criteria and thermal criteria, selection of protection systems, such as blocking diodes, fuses, load disconnectors, surge protection devices (SPD), and compliance with grid connection standards. Finally, a techno-economic analysis is performed, calcu-

lating the Levelized Cost of Electricity (LCOE). A financial amortization plan is developed to assess investment feasibility, and an environmental impact assessment estimates the GHG emissions reduction achievable with the proposed system. Additional environmental concerns related to large-scale PV deployment are also discussed.

This study provides a comprehensive framework for the optimal design of large-scale PV power plants, integrating technical, economic, and environmental perspectives to support sustainable energy development.

References

[1] U-Energy. Doped silicon p-type and n-type junction.

[2] U-Energy. Pn-junction in photovoltaic cells.

[3] Filippo Spertino. Renewable energy systems lessons, 2023. Academic Year 2023.

[4] SMA Solar Technology. *Sunny Central 2000 / 2475 Inverter Manual*, 2022.

[5] International Renewable Energy Agency (IRENA). Renewable power generation costs in 2023. Technical report, International Renewable Energy Agency, Abu Dhabi, 2024.

[6] Ana Cabrera-Tobar, Eduard Bullich, Monica Aragüés-Peñalba, and Oriol Bellmunt. Topologies for large scale photovoltaic power plants. *Renewable and Sustainable Energy Reviews*, 59:309–319, 06 2016.

[7] Comitato Elettrotecnico Italiano (CEI). Cei 0-16: Reference technical rules for the connection of active and passive consumers to the lv electrical utilities, 2019.

[8] ENTSO-E. Entso-e tso grid map, 2024.

[9] Ettore Bompard, Tao Huang, and Daniele Grosso. E-transition sustainability and economics lessons, 2023. Academic Year 2023/2024 Politecinco di Torino.

[10] Terna S.p.A. Revisione configurazione zonale - report finale. Technical report, Terna S.p.A., Marzo 2018.

[11] C. Schwingshackl, M. Petitta, J.E. Wagner, G. Belluardo, D. Moser, M. Castelli, M. Zebisch, and A. Tetzlaff. Wind effect on pv module temperature: Analysis of different techniques for an accurate estimation. *Energy Procedia*, 40:77–86, 2013. European Geosciences Union General Assembly 2013, EGUDivision Energy, Resources & the Environment, ERE.

[12] ABB. *ABB Photovoltaic Guide*, N.D.

[13] International Energy Agency (IEA). Italy 2023 energy policy review, 2023.

[14] PennState University. Pv technology report, N.D.

[15] LONGi Solar. *Installation Manual for LONGi Solar PV Modules*, 2023.

[16] R. Josephs. *Solar Cell Array Design Handbook*. NASA, Washington, DC, USA, 1976.

[17] Weidong Xiao, W.G. Dunford, and A. Capel. A novel modeling method for photovoltaic cells. In *2004 IEEE 35th Annual Power Electronics Specialists Conference (IEEE Cat. No.04CH37551)*, volume 3, pages 1950–1956 Vol.3, 2004.

[18] Ahmed El Tayyan. A simple method to extract the parameters of the single-diode model of a pv system. *Turkish Journal of Physics*, 37:121 – 131, 03 2013.

[19] Tofopefun Olayiwola, Seung Hyun, and Sung-Jin Choi. Photovoltaic modeling: A comprehensive analysis of the i–v characteristic curve. *Sustainability*, 16:432, 01 2024.

[20] SMA Solar Technology. *Central Inverter Planning of a PV Generator: Planning Guidelines*, 2017.

[21] NASA. Nasa power access data viewer, 2024.

[22] 3Bmeteo. Historical weather data for guglionesi, 2012.

[23] PVGIS - European Commission Joint Research Centre. Pvgis - photovoltaic geographical information system, 2024.

[24] E. Skoplaki, A.G. Boudouvis, and J.A. Palyvos. A simple correlation for the operating temperature of photovoltaic modules of arbitrary mounting. *Solar Energy Materials and Solar Cells*, 92(11):1393–1402, 2008.

[25] SunEarthTools. Sun position calculator, N.D.

[26] Soteris A. Kalogirou Arno Smets Klaus Jäger Olindo Isabella René van Swaaij Miro Zeman. *Solar Energy Engineering: Processes and Systems*. Academic Press, 2023.

[27] Electricity Maps. Real-time carbon intensity of electricity in italy (it), 2023. Accessed: 2023-10-10.

A Implementation of the V-I Curve Model in MATLAB

Below there is the MATLAB code used to generate the results. It uses the exponential two parameter analytical-based approximation of a PV module.

```
clear  % Clear all variables in the workspace
Pmax=620;  % Maximum power of the photovoltaic module
Vmp=44.55;  % Voltage at maximum power point
Imp=13.92;  % Current at maximum power point
Voc_stc=52.66;  % Open-circuit voltage under STC conditions
Isc_stc=14.81;  % Short-circuit current under STC conditions
eta=0.23;  % Module efficiency
etaVoc=-0.23/100;  % Temp. coeff. of open-circuit voltage
etaIsc=0.045/100;  % Temp. coeff. of short-circuit current
etaPmax=-0.28/100;  % Temp. coeff. of maximum power
T_STC=25;  % Reference temperature (gradi C)
G_STC=1000;  % Reference irradiance (W/mq)
Rs=8*10^(-3);  % Series resistance of the module (36 mohm)
G=[200, 400, 600, 800, 1000]; % Irradiance vector  [W/mq]
DeltaI=zeros(length(G));  % vector for current variations
DeltaV=zeros(length(G));  % vector for voltage variations
Isc=zeros(length(G));  % vector for short-circuit currents
Voc=zeros(length(G));  % vector for open-circuit voltages
C2=(Vmp-Voc_stc)/log(1-Imp/Isc_stc);
C1=Isc_stc/(1-exp(-Voc_stc/C2));  % Calculate parameter C1
% Update Isc and Voc based on irradiance variation (G)

for i=1:length(G)
    DeltaI(i)=Isc_stc*(G(i)/G_STC-1)+etaIsc*(G(i)/G_STC)*(
        T_STC-T_STC);  % I_sc variation due to G
    Isc(i)=Isc_stc+DeltaI(i);  % New short-circuit current
    DeltaV(i)=etaVoc*(T_STC-T_STC)-Rs*DeltaI(i);
    Voc(i)=Voc_stc+DeltaV(i);  % New open-circuit voltage
end

V=linspace(0,55,5000);  % Voltage vector from 0 to 55 V
PV_I=real(zeros(length(V)+1,length(G)));  % matrix for PV
    currents

% Calculate PV current for each combination of voltage and
    irradiance
for i = 1:length(V)
    for j = 1:(length(G) + 1)
        if j == 1
            PV_I(i, j) = 0;
        else
            PV_I(i, j) = Isc(j - 1) - C1 * exp(-Voc(j - 1) /
                C2) * (exp(V(i) / C2) - 1);
```

```
40
41              if PV_I(i, j) < 0
42                 PV_I(i, j) = NaN;
43              end
44          end
45      end
46  end
47
48  % Extract the last column of PV_I
49  I_G1000 = PV_I(1:5000, end);  % Use only the first 5000
        elements for compatibility with V
50  I_G1000 = I_G1000';  % Transpose I_G1000 to make it a row
        vector (1x5000)
51
52  % Calculate power P = V .* I_G1000 (element-wise product)
53  P = V .* I_G1000;  % P will be a row vector 1x5000
54
55  % Plot I-V curves for different irradiance values (G)
56  I=Isc(1)-C1*exp(-Voc(1)/C2)*(exp(V/C2)-1);  % Current for
        the first value of G
57   if I(I<0)<0
58      I(I<0) = NaN;  % Set to NaN if current is negative
59   end
60  plot(V,I,'b');  % Plot I-V curve for G=200 W/mq (blue)
61  hold on  % Keep the graph active to overlay curves
62
63  I=Isc(2)-C1*exp(-Voc(2)/C2)*(exp(V/C2)-1);  %
64  if  I(I<0)<0
65      I(I<0) = NaN;  % Set to NaN if current is negative
66   end
67  plot(V,I,'r');  % Plot I-V curve for G=400 W/mq (red)
68
69  I=Isc(3)-C1*exp(-Voc(3)/C2)*(exp(V/C2)-1);
70  if I(I<0)<0
71     I(I<0) = NaN;  % Set to NaN if current is negative
72   end
73  plot(V,I,'g');  % Plot I-V curve for G=600 W/mq (green)
74
75  I=Isc(4)-C1*exp(-Voc(4)/C2)*(exp(V/C2)-1);
76   if I(I<0)<0
77      I(I<0) = NaN;  % Set to NaN if current is negative
78   end
79  plot(V,I,'y');  % Plot I-V curve for G=800 W/mq (yellow)
80
81  I=Isc(5)-C1*exp(-Voc(5)/C2)*(exp(V/C2)-1);
82  if I(I<0)<0
83     I(I<0) = NaN;  % Set to NaN if current is negative
84   end
85  plot(V,I);  % Plot I-V curve for G=1000 W/mq (default color)
86
```

```
I=Isc(6)-C1*exp(-Voc(6)/C2)*(exp(V/C2)-1);
if  I(I<0)<0
    I(I<0) = NaN;  % Set to NaN if current is negative
 end
plot(V,I);  % Plot I-V curve for G=1000 W/mq (default color)

%plot(V, P, 'b', 'LineWidth', 2);  % Plot P-V curve in blue

yyaxis left;  % Activate left y-axis for current
plot(V, I, 'r', 'LineWidth', 2);  % I-V curve in red
ylabel('Current I [A]');  % Label for left y-axis
ylim([0, 20]);  % Set limits for left y-axis

yyaxis right;  % Activate right y-axis for power
plot(V, P, 'b', 'LineWidth', 2);  % P-V curve in blue
ylabel('Power P [W]');  % Label for right y-axis
ylim([0, max(P)*1.1]);  % Set limits for right y-axis

% Add labels, title, and grid
xlabel('Voltage V [V]');  % Label for x-axis
title('I-V and P-V Curves for G = 1000 W/mq');
%legend('I-V Curve', 'P-V Curve');  % Legend

% Find the maximum power point (MPP)
[etaPmax, idx] = max(P);  % Max value of P and its index
Vmp = V(idx);  % Voltage at maximum power point

% Add MPP point to the graph
plot(Vmp, etaPmax, 'ko', 'MarkerSize', 2.5, 'LineWidth', 2);
      % Maximum power point (MPP) comment to see only
text(Vmp + 1, etaPmax - 5, sprintf('MPP: %.2f W', etaPmax),
    'FontSize', 12);  % MPP annotation
```